SERI/TR-8041-9-T1

FABRICATION AND TESTING OF MIS SOLAR CELLS ON a-Si:F:H

Final Report for Period September 15, 1979—September 15, 1980

By
Min-Koo Han
Wayne A. Anderson

November 3, 1980

Work Performed Under Contract No. AC02-77CH00178

The State University of New York at Buffalo
Department of Electrical Engineering
Amherst, New York

U.S. Department of Energy

Solar Energy

DISCLAIMER

DISCLAIMER

SERI/TR-8041-9-T1
Distribution Category UC-63

Wayne A. Anderson, Principal Investigator
The State University of New York at Buffalo
Department of Electrical Engineering
4232 Ridge Lea Road
Amherst, New York 14226

FINAL REPORT

FABRICATION AND TESTING OF MIS SOLAR CELLS ON a-Si:F:H

September 15, 1979 - September 15, 1980

Written by

Min-Koo Han

and

Wayne A. Anderson

November 3, 1980

Sponsored by

Solar Energy Research Institute
Photovoltaic Program Office
1617 Cole Boulevard
Golden, Colorado 80401

Contract No. XS-9-8041-9

Administered by

Southeastern Center for Electrical Engineering Education
Central Florida Facility
1101 Massachusetts Avenue
St. Cloud, Florida 32769

ABSTRACT

Fabrication techniques and improved a-Si:H film processing have been achieved to produce a short circuit current density of 7.5 mA/cm^2 and open circuit voltage of 740 mV on large area (2cm^2) a-Si cells by the deposition of an inexpensive semitransparent metal (Cr) as a top electrode on a N-I-P structure. This corresponds to a 2% efficiency using AM1 illumination. A V_{oc} of 830 mV and fill factor of 0.54 have also been separately obtained. A relatively simple and inexpensive deposition technique using a one pump-down vacuum system, Al grid and thin metal film structure have been applied to reduce the cost of a-Si:H cell fabrication.

A SEM study of a-Si film quality shows the substrate texture to greatly influence the film morphology. This in turn serves to influence the uniformity of photovoltaic response on completed solar cells.

The studies of optical transmittance of various thin metal films promote the utilization of Cr and Cu as a top electrode. Cr and Cu are promising materials for N-I-P a-Si:H films. In P-I-N films, V_{oc} of Pd cells is larger than Cr cells while J_{sc} of Cr cells is better than Pd cells. Optical studies of our a-Si films give an absorption coefficient in agreement with other workers.

For a P-I-N structure, Cr gives $V_{oc} \approx 550$ mV whereas Pd gives $V_{oc} \approx 650$ mV since Pd has a higher ϕ_m giving a better ohmic contact to P-Si. For a N-I-P structure, Cr gives $V_{oc} \approx 800$ mV whereas Pd gives $V_{oc} \approx 750$ mV since Cr has a lower ϕ_m giving a better ohmic contact to P-Si. When considering a N-I structure, the higher ϕ_m of Pd gives increased V_{oc} over Cr since the I-layer is somewhat n-type.

Dark and illuminated I-V characteristics show that current conduction mechanisms and recomination pheonomena are not the same under dark and illuminated conditions. Furthermore, spectral response analysis and reverse illuminated saturation current under different illumination levels show photoconductivity and collection efficiency to be a function of illumination level. Significant differences in spectral response on observed when comparing P-I-N, N-I-P and I-N structures. A Schottky barrier lowering effect is proposed to explain some spectral response data. The importance of the top junction region to carrier collection is also discussed.

TABLE OF CONTENTS

LIST OF FIGURES

TABLE

1. INTRODUCTION AND RESEARCH STATEMENT

1-1 Introduction

During the past year, the direction of our work has been focused on five fundamental conditions for efficient photovoltaic energy conversion. Five basic requirements to improve photovoltaic performance are: 1) large optical absorption, 2) reasonable collection efficiency, 3) large built-in-potential, 4) low resistance, and 5) good film uniformity. Three parameters determining the efficiency of solar cells, short circuit current density (J_{sc}), open circuit voltage (V_{oc}) and fill factor (FF) are controlled by those five conditions.

A significant fraction of photons must be absorbed in the thin Si film. More than 95% of the visible portion of an AM1 solar spectrum will be absorbed in an a-Si film of 1 μm thickness. Photogenerated electrons and holes due to absorbed photons must be collected by conducting material at the top and bottom of a-Si films through drift and diffusion processes. The operating voltage of solar cells is strongly controlled by a built-in-potential. Built-in-potentials also determine the depletion width and amount of drift field. Since the major conduction mechanism in a-Si solar cells is a drift process rather than the diffusion of minority carriers,[1,2,3] which is the dominant conduction mechanism in single or poly-cyrstalline solar cells, the built-in-potential will strongly influence the short circuit current density. Series resistance must be small to reduce the loss of output voltage during operation of photovoltaic devices.

Short circuit current density is directly controlled by conditions 1 and 2. Open circuit voltage is related to conditions 3 and 5. Series resistance and film uniformity control fill factor. The drift field, which is related to the built-in-potential, also controls the fill factor in a-Si solar cells. This phenomena is similar to the fact that in single crystalline Si cells, fill factor is controlled by diffusion length.[4]

The relationships between cell parameters and the five conditions have not been identified fully but some possible factors are substrate temperature, substrate material and surface finish, doping parameters, dimensions or cell structure (thickness of N-I-P layers), back contact (substrate) and front contact (S.B. metal, A/R coating and grid structure).

The specific goals of our research are listed below:

1) Identify conduction mechanisms in a-Si cells.

2) Optimize the interfacial layer to obtain a stable and high V_{oc}.

3) Investigate hole trapping effects.

4) Investigate surface-state behaviour.

5) Study diffusion length data and recombination data as a function of fabrication parameters .

6) Identify the contribution of cell parameters to the fundamental requirements of a-Si solar cells.

7) Improve J_{sc} and FF as result of (1) - (3) above.

1-2. Research Statement

Uniform and reproducible films are important requirements for a-Si solar cells. Our films are mainly supplied by John Coleman of Plasma Physics Corporation. Different glow discharge environments for P-I-N, N-I-P and I-N structures have been applied by John Coleman and different types of Schottky barrier metals have been deposited on these films.

Film studies have been performed through X-ray scan and SEM analysis to investigate quality of these films. The effective optical absorption coefficient of P-I-N layers and of undoped layers has been obtained. Cleaning procedures for a-Si films have been established. A newly designed mask makes it possible to test for film uniformity, the effect of cell area on photovoltaic performance, and degree of optimization of the A/R coating. A one pump-down vacuum process has been used for depositing several materials.

To characterize collection and recombination mechanisms, spectral response analysis at various illumination levels under forward bias and reverse conditions have been performed. Standard photovoltaic tests for V_{oc}, J_{sc} and FF are made on all cells. These data are then related to the fabrication process in order to determine an optimum process for film deposition and for final device design. I-V-T, C-V-f, and G-V-f data are being obtained to evaluate conduction mechanisms and built-in potentials. The goal of this study is to relate processing variables to conduction mechanisms in an effort to optimize solar cell design.

2. FILM AND SUBSTRATE STUDIES

2-1. Quality and Uniformity of a-Si Films

Uniform a-Si film quality and thickness have been major obstacles in producing good and consistent a-Si solar cells. SEM analysis and X-ray scan have been performed to investigate a-Si film quality. A-Si films with many cracks and pinholes (Figure 1-a) have shown very inconsistent and poor photovoltaic performance or have been shorted, probably due to the coarse structure. Improved photovoltaic response has been obtained from a-Si films having better uniformity. We show that 7.5 mA/cm^2 short circuit current density (internal current = 11.5 mA/cm^2) and 803 mV open circuit voltage have been produced from the improved films (Figure 1-b). An SEM picture clearly shows that quality and uniformity of the film is not quite satisfactory.

Since a-Si:H solar cells are truly thin film devices (thickness of the film is less than 1 μm), the roughness of an unpolished substrate surface can be easily on the order of the film thickness. Uniformity of the a-Si is very important to performance compared with thick film cells. A uniform structure can be seen in a-Si films deposited on a highly polished stainless steel substrate shown in Figure 1-c. An X-ray scan also indicates that the thickness of an a-Si film on an unpolished polished stainless steel is not uniform. X-ray scan data for a void area show the presence of elements commonly found in a stainless steel substrate meaning that shorting will occur in devices made from this structure. To improve the photovoltaic performance of a-Si solar cells, the nature of the substrate is very important. There could also be an oxide layer on the surface of the substrate

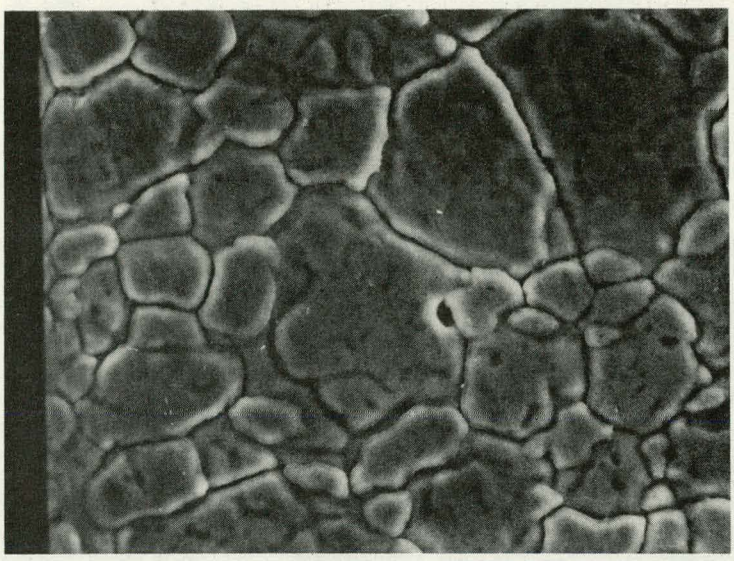

Figure 1-a. SEM Micrograph of a-Si Film Deposited on Unpolished Stainless Steel. (1000X)

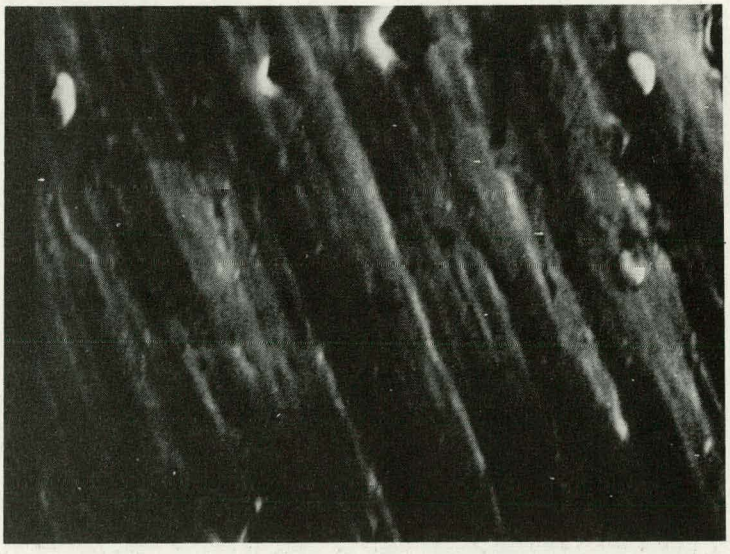

Figure 1-b. SEM Micrograph of Improved a-Si Film Deposited on a Unpolished Stainless Steel having a Better surface. (3000X)

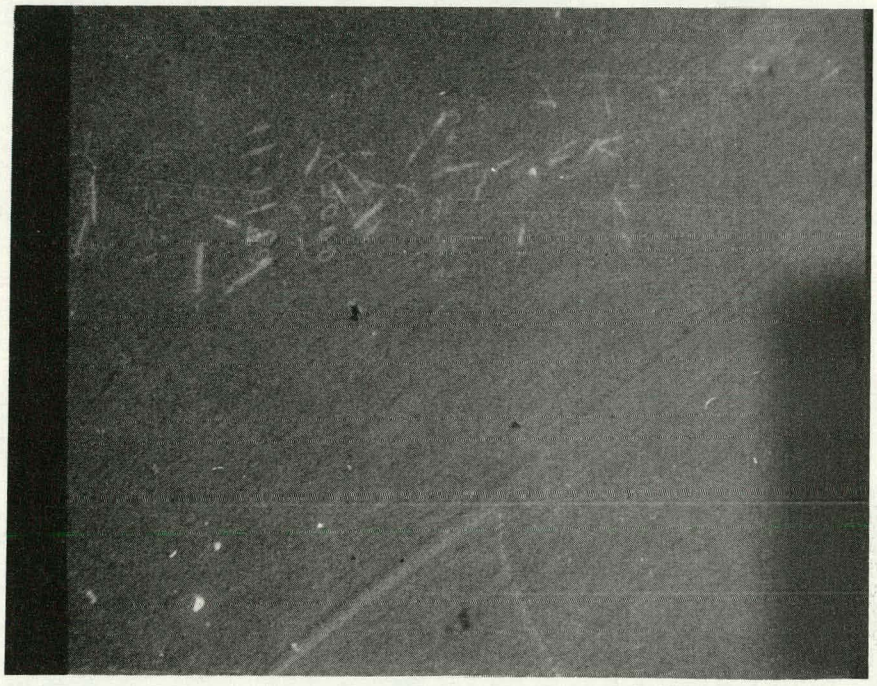

Figure 1-c. SEM micrograph of a-Si film on polished stainless steel (3000X).

which can change the contact resistance. Polished and chemically cleaned stainless steel as a substrate may significantly improve our existing photovoltaic response.

The growth kinetics of a-Si:H film and contact resistance can be altered by the properties of the substrate. a-Si:H films have been deposited on stainless steel and Mo substrates under identical glow discharge environments. Neither substrate was polished but films on a Mo substrate show a more uniform structure (Figure 2-a) except for some columnar growth. Roughness and pin-holes can be seen on a-Si:H films on stainless steel substrates as shown in Figure 2-b. Figures 3-a and 3-b show more detailed information on the surface structure by utilizing a Y-mode scan of the SEM. Photovoltaic measurements also indicate the improvement in quality and uniformity of a-Si:H films on the Mo substrate. A significant increase of fill factor, from 0.35 on stainless steel substrate to 0.45 on Mo substrate, was observed while J_{sc} and V_{oc} were almost the same.

Film quality also affects the diode quality factor (n) and shunt resistance. Shunt resistance has been very low and the diode quality factor n is more than 5 in poor quality films probably due to pin-holes or non-uniform thickness of the film. The effect of shunt resistance due to poor quality of film will be discussed later.

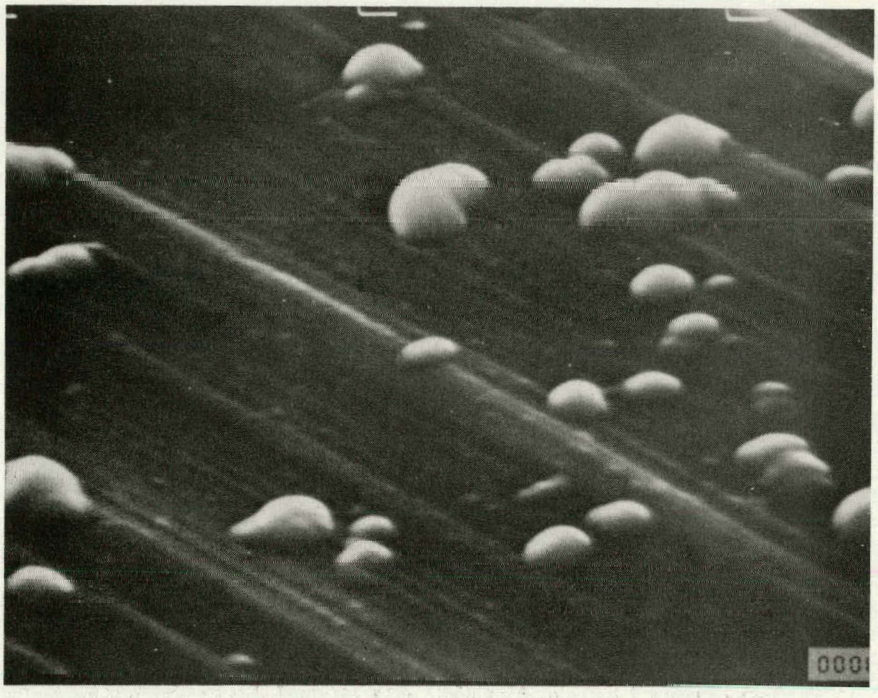

Figure 2-a. SEM micrograph of a-Si film on unpolished Mo (5000X).

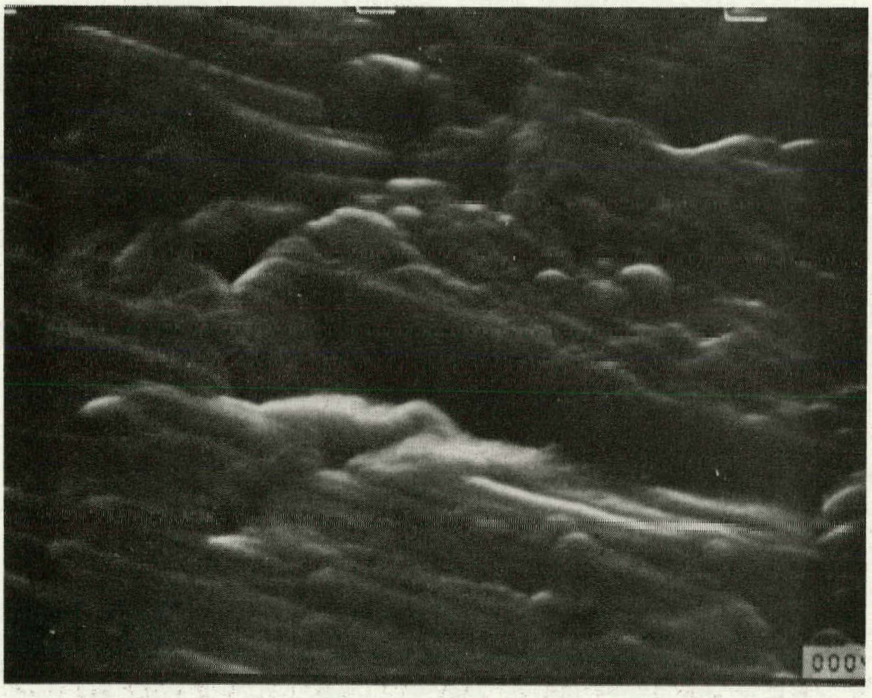

Figure 2-b. SEM micrograph of a-Si film on unpolished stainless steel (5000X).

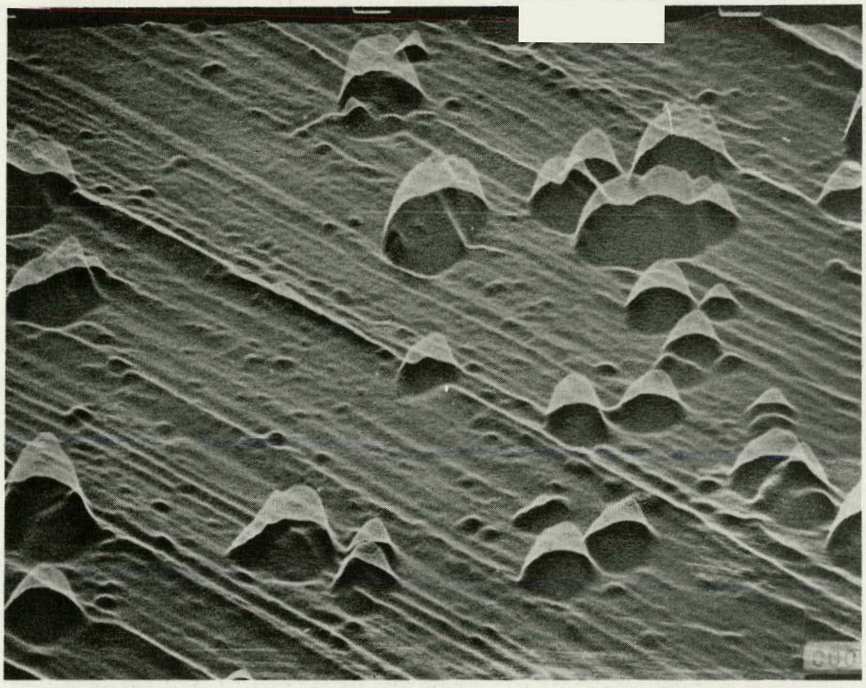

Figure 3-a. SEM line scan of sample in Figure 2-a. (5000X).

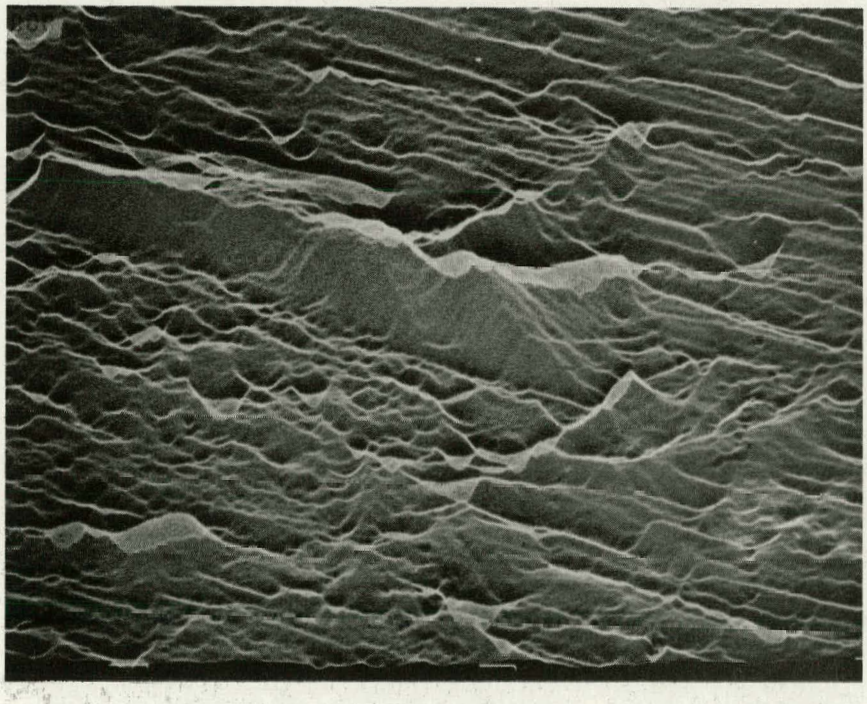

Figure 3-b. SEM line scan of sample in Figure 2-b (5000X).

2-2. Thickness of a-Si:H Films

The measurement of film thickness is probably the first step to characterize a-Si:H films. An accurate evaluation of deposition rate and optical absorption coefficient (α) is dependent on the estimation of film thickness. A widely used technique to measure thin film thickness utilizes the inteference effect. The refractive index of samples must be known in the inteference measurement. Since the refractive index of a-Si:H films is not well established, we have used an SEM measurement rather than the inteference effect.

There is a sharp boundary between substrate and film near the edge of the sample due to the deposition procedure used in a-Si work. We examined this sharp boundary by tilting the sample and using a magnification of 3000-5000X. Thickness of the sample is easily obtained by,

$$W_s = \frac{W_{SEM}}{\text{Magnification}} \times \cos(90°\text{-tilted angle}) \ . \qquad (2\text{-}1)$$

This very simple and nondestructive testing provides a measurement of thickness of thin film devices. Deposition rate is then easily obtained from thickness. Some SEM pictures of this boundary are shown in Figure 4. Figures 4-a and 4-b show the edge view for deposition times of 1 hour and 2 hours, respectively. Thicknesses of 0.5 μm and 1.0 μm are calculated from these figures.

2-3. Optical Properties of a-Si:H Films

The optical absorption and bandgap energy are very important parameters to determine the photovoltaic performance of a-Si:H solar cells. The short circuit current density is dependent on the optical properties of a-Si:H films. Information on the absorption coefficient is essential to analyze the current collection mechanisms from the spectral response data.

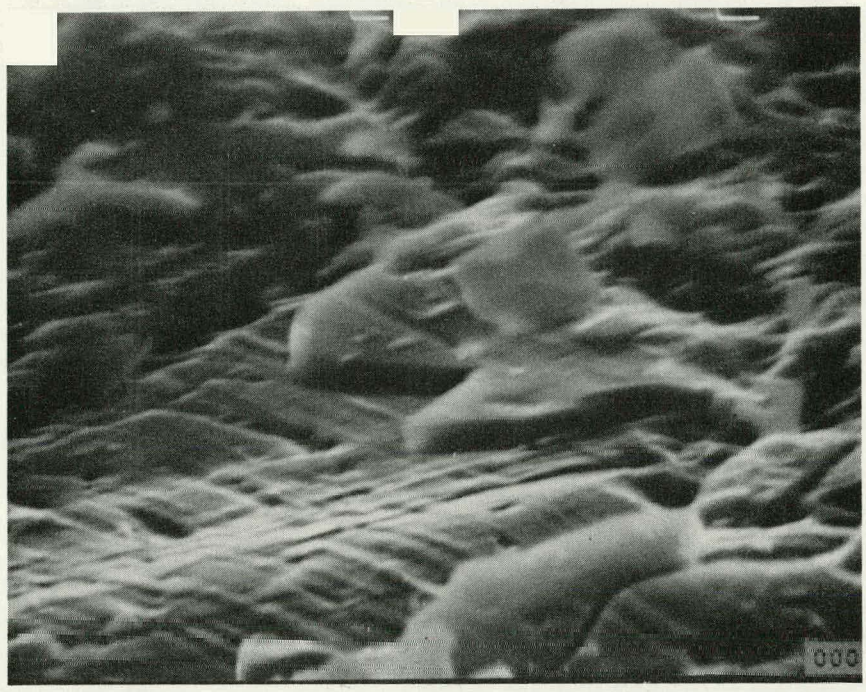

Figure 4-a. SEM micrograph showing a-Si film edge for 1 hour deposition (5000X).

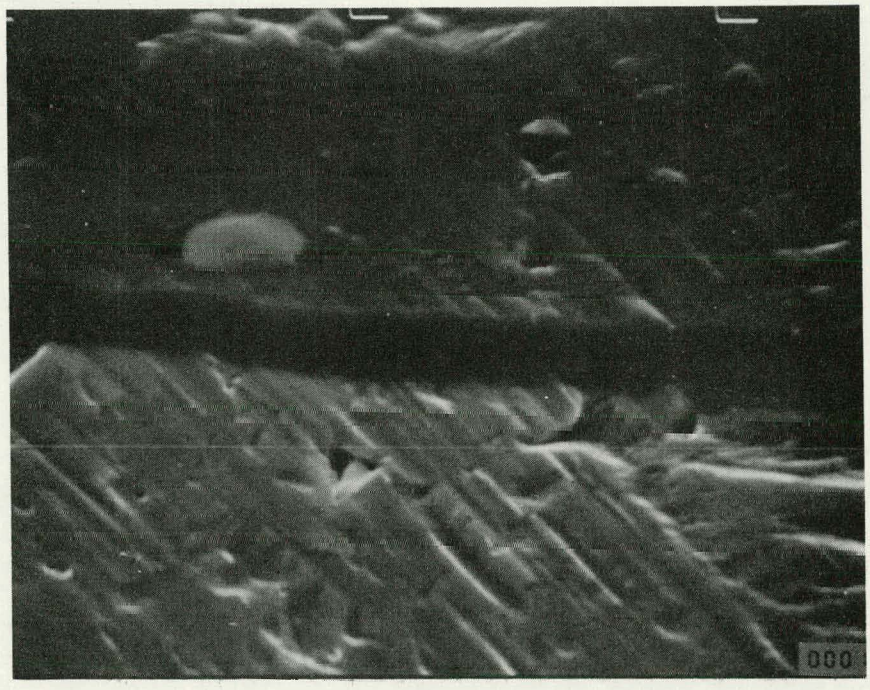

Figure 4-b. SEM micrograph showing a-Si film edge for 2 hours deposition (5000X).

The UV-visible absorption coefficient for discharge-produced a-Si:H films are calculated from transmittance data obtained by a GCA/Mcpherson, EU-700 series, double-beam scanning spectrophotometer, equipped with a recorder and digital controller.

The absorption coefficient was calculated by utilizing

$$T = \frac{I_o}{I_{in}} = \exp(-\alpha(\lambda) \cdot D) \qquad (2\text{-}2)$$

where

T = Transmittance

$\alpha(\lambda)$ = Absorption Coefficient

D = Thickness of Sample.

The thickness of samples was calculated from the deposition rate obtained by SEM measurement as outlined in the previous section. Three different samples were tested having film thicknesses of 0.15 μm, 0.3 μm, 0.45 μm. These samples were composed of an undoped layer deposited on glass with a substrate temperature of 250° C. A linear variation of $\sqrt{\alpha h\nu}$ vs $h\nu$ was observed and optical energy bandgap around 1.65 eV was obtained as shown in Figure 5. An American Instrument Model PM-2 spectrophometer was used to confirm this result. Figure 6 shows a α vs $h\nu$ of a a-Si:H and single crystalline silicon for comparison.

Figure 5. Optical Bandgap Determination in Undoped a-Si.

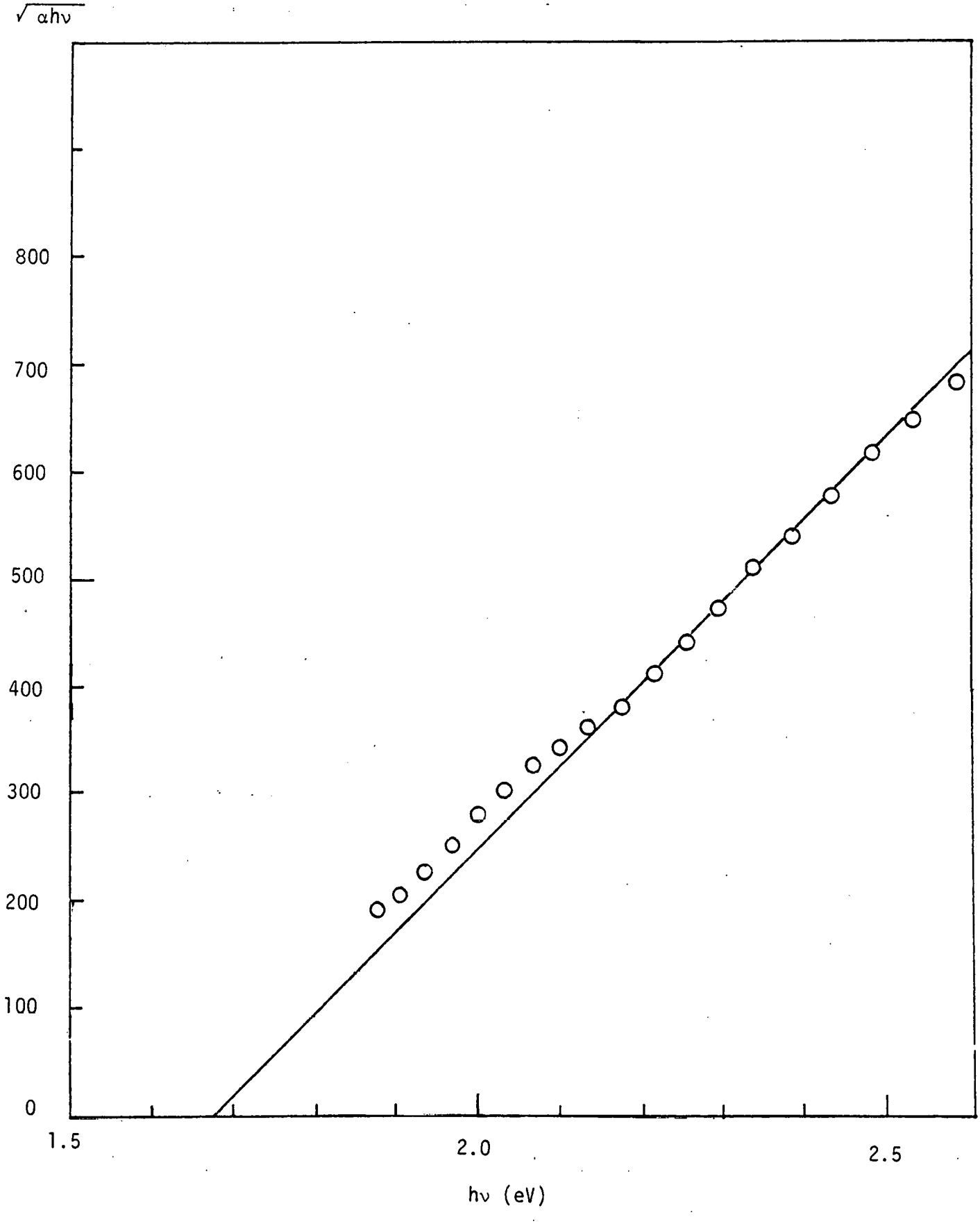

Figure 6. Absorption Coefficient in Undoped a-Si.

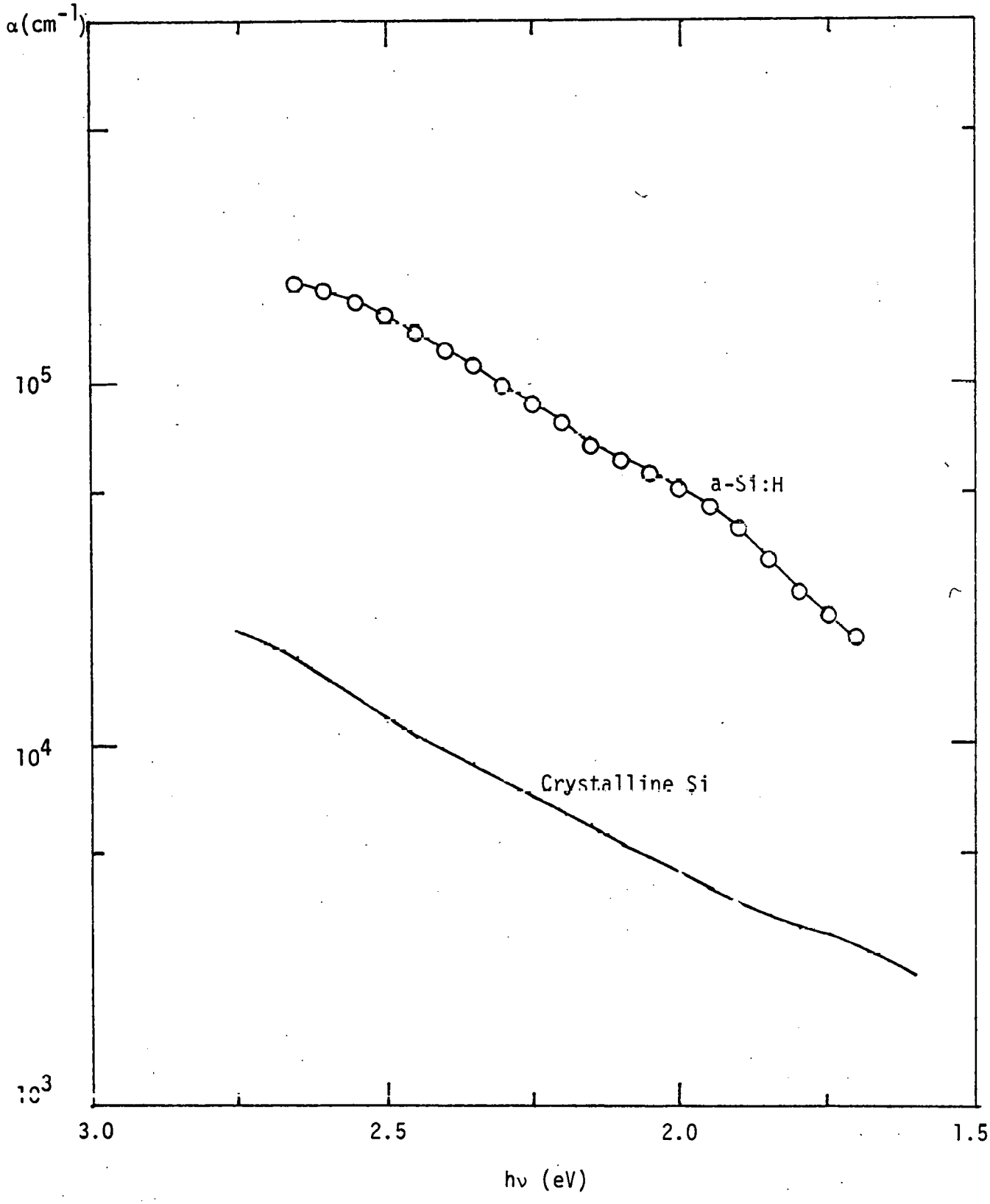

3. FABRICATION OF SOLAR CELLS ON a-Si:H

Most of our a-Si:H films were provided by John Coleman of Plasma Physics Corporation. We have investigated the quality and uniformity of these films and have measured the film thickness as outlined in Chapter 2. We have fabricated solar cells utilizing various electrodes prior to testing and analysis.

Large area (200 cm^2) a-Si:H films were formed on various substrates (stainless steel, Cr, Al, Mo) utilizing a d.c. glow discharge decomposition of silane with doping by phosphine or diborine to form n or p type layers. A flow rate of 200 cc/min of 5% silane in helium and a pressure of 2 Torr were maintained in the system. The substrates were held at various temperatures (200-350° C) on the cathode using a resistance heater. The deposition time of 1 hour leads to a undoped film thickness of approximately 0.5 μm, corresponding to our average deposition rate of around 1.5 $\mathring{A}\ s^{-1}$ for a substrate temperature of 250° C. The a-Si:H film cell structure consists of a few hundred angstroms of boron or phosphorous doped layer, 0.5 - 1 μm of undoped layer, and a few hundred angstroms of phosphorous or boron doped layer.

a-Si silms have been exposed to air more than 48 hours before fabrication. These films are cleaned in acetone and deionized water then blown dry using a dry N_2 steam. Three different types of a-Si:H solar cells have been fabricated, Schottky barrier structure (-I-N-substrate), P-I-N and N-I-P-substrate structure. These solar cells have a structure of grid metal/electrode (Schottky barrier metal in case of I-N-substrate structure)/a-Si:H films/metal substrate as seen in Figure 7. 30-100 $\mathring{A}$ of various metals (Pd, Cr, Cu, Ht, Ag) were evaporated to make a semitransparent, highly conductive layer for rectifying contacts (in the case of

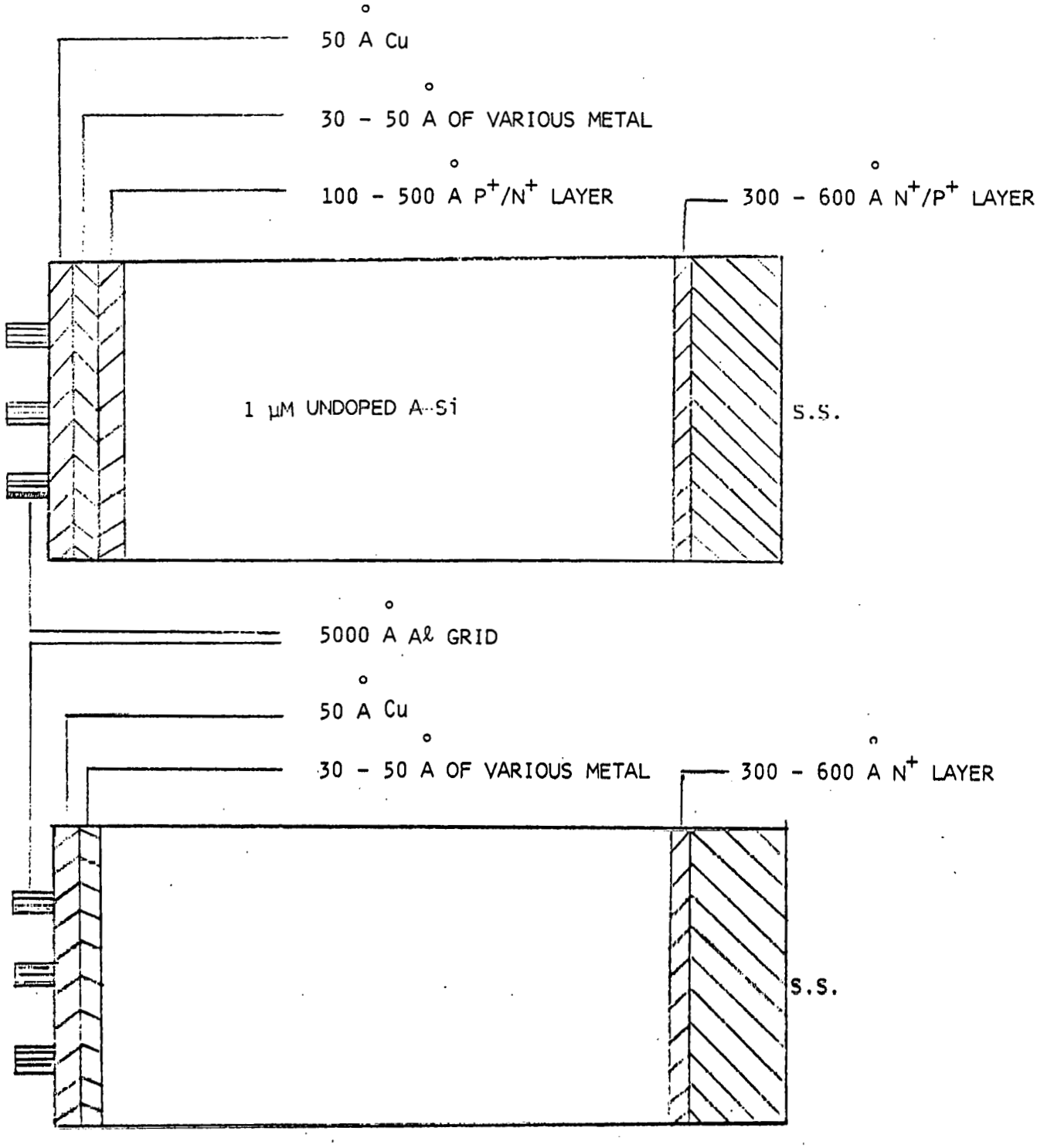

Figure 7. Solar Cell Structure

P-I-N or N-I-P films) and Schottky barrier metal (for I-N films). When using Cr, Pd and Hf films, about 50 Å of Cu were deposited over the initial metal to reduce the sheet resistivity of the top electrode. Although the work function of Cu is low, optical transmission ability is very high and sheet resistivity is also quite good.

Optical transmittance and resistivity of the thin metal films were measured by depositing the thin metal films simultaneously on Corning precleaned microslides. Internal current, which is widely used to determine the quality of a-Si:H solar cells, can be obtained quite reliably from the external current. The top layers are deposited in one pump-down using a special vacuum system. This vacuum system includes a special fixture permitting the use of six different substrates, six different masks and six different evaporation sources. A thickness monitor and substrate heater are also included in the system. A minimum thickness of 30 Å Cr and 50 Å Pd is required to deposit a continuous film.[5]

A newly designed mask, shown in Figure 8, is used to fabricate 11 different cells with active areas from 0.04 cm^2 to 2 cm^2. Some advantages of this mask are that uniformity and quality of each film can be studied and the effect of area on photovoltaic performance (i.e. fill factor) can also be analyzed. An A/R coating has not been applied to all cells so that comparison of cells with A/R coating and without A/R coating provides information about its influence on J_{sc}. A 20 $\sim$ 25% increase in J_{sc} with A/R coating was observed. An optimized A/R coating can be expected to give a 50 $\sim$ 60% increase in J_{sc}.

Figure 8. Diagram of Sample and Mask.

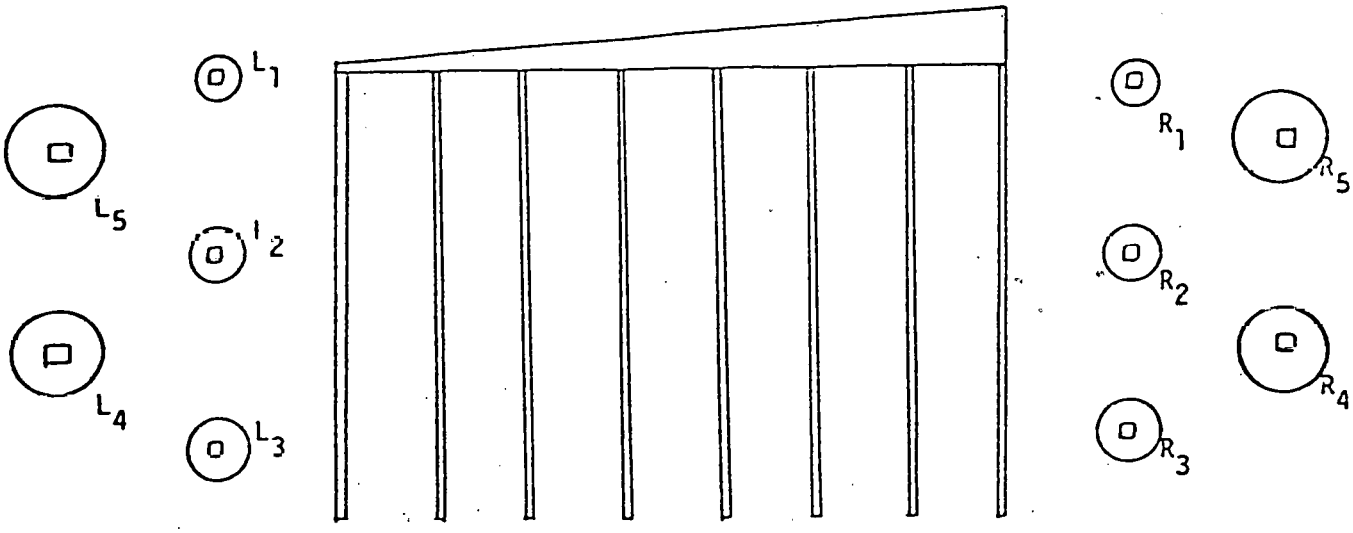

Cell	Total Area (cm^2)	Active Area (cm^2)
L_1, R_1	0.4	0.026
L_2, R_2	0.08	0.066
L_3, R_3	0.10	0.086
L_4, R_4	0.15	0.136
L_5, R_5	0.20	0.186
Middle Cell	2.42	2.00

4. PERFORMANCE OF a-Si:H SOLAR CELLS

More than 80 cells have been fabricated, tested and analyzed during the course of the present work. The cells have been characterized on the basis of the measurements including both dark and illuminated I-V characteristics, variation of short circuit current density and open circuit voltage at different illumination levels. Performance data for pertinent cells are listed in Table I. The photovoltaic measurements were performed under AM1 illumination at room temperature. AM1 illumination environment was simulated by an ELH lamp for which the intensity was adjusted by calibrating the short circuit current for a NASA-Lewis standard P-N junction silicon solar cell.

J_{sc} = 7.5 mA/cm^2 (internal short circuit current = 11.5 mA/cm^2) V_{oc} = 745 mV, and an efficiency of 2% were produced on a large area cell (2 cm^2) which utilized inexpensive materials such as 30 Å Cr and 50 Å Cu as top electrodes on N^+-I-P^+-stainless steel structures. Transmittance (T_m) of the top electrode was 66% and resistivity (ρ_m) was 110 Ω/[]. V_{oc} > 800 mV and FF > 0.5 were produced separately on other cells with Cr as a top electrode.

As discussed in Chapter 3, three different type of cells were studied; Schottky barrier, P-I-N and N-I-P. V_{oc} of Schottky barrier cells with Cr and Pd are 20-50% higher than previously reported results. The slope of $\Delta V_{oc}/\Delta\phi_m$ is almost the same as in previously reported results. It is clear that a high work function metal is desired to produce a high V_{oc} and J_{sc} in Schottky barrier type cells utilizing undoped a-Si:H. Schottky barrier a-Si:H cells thus far have required very expensive materials as a Schottky metal to produce V_{oc} of more than 550 mV.[6,7] The highest V_{oc} previously reported on a Schottky barrier cell is 803 mV[8] using a Pt

PHOTOVOLTAIC PERFORMANCE AND PROPERTIES OF a-Si:H SOLAR CELLS MEASURED AT AM1 (100 mW/cm^2) AND 28° C.

TABLE I

Cell #	Film #	Cell Configuration	Tr (%)	$\rho_m(\Omega/[])$	$J_{sc}(\frac{mA}{cm^2})$	V_{oc}(mV)	FF	Eff (%)
43	45	Cr-P-I-N-SS	51	110	3.8	560	0.38	0.80
44	45	Pd-P-I-N-SS	40	42	3.7	660	0.38	0.92
47	105	Cr-N-I-P-Mo	71	100	4.6	800	0.45	1.65
50	105	Pd-N-I-P-Mo	55	880	3.6	755	0.45	1.21
54*	182	Cr-N-I-P-SS	66	340	3.5	788	0.32	0.85
55*	182	Pd-N-I-P-SS	37	60	3.1	762	0.30	0.70
32**	140	Cr-N-I-P-SS	66	110	7.5	745	0.36	2.01
5	48	Pd-I-N-SS	-	-	4.2	475	0.41	0.82
13	48	Cr-I-N-SS	-	-	4.0	320	0.39	0.80

* Very heavily doped N layer (10% PH_3/SiH_4)

** Best cell made thus far and only one with an antireflection coating. (Area = 2 cm^2)

electrode. The stability of Schottky barrier cells is not yet well established.

Our main effort now involves P-I-N or N-I-P structures to utilize the advantages of a high built-in potential. Advantages of P-N junction cells over Schottky barrier type cells lie in the fact that junction properties can be easily controlled continuously during the film deposition, possibly greater stability[9,10] and a large inherent built-in-potential (greater than 1.1 eV).[11,12] Fabrication of the a-Si:H P-I-N junction structure is relatively simple and does not require any costly processing, unlike crystalline or polycrystalline devices. Metal work function of the top electrode partially controls the V_{oc}. V_{oc} of P-I-N cells utilizing a higher work function metal (Pd) is smaller than V_{oc} of cells with identical films when using lower work function metal (Cr, Al, Cu, Ag). V_{oc} of N-I-P cells using a higher work function metal (Pd) is larger than V_{oc} of cells utilizing lower work function metal (Cr). Typical values of V_{oc} are 760 mV on Cr, Cu and Al cells and 700 mV on Pd cells utilizing P-I-N films. V_{oc}= 600 mV for Pd cells and 540 mV for Cr cells on N-I-P films were typical.

Photovoltaic performance and properties of thin metal films of Cr and Pd on identical a-Si:H films are listed in Table I. Thickness of Cr, Pd and Cu are 30 Å ± 5%, 40 Å ± 5% and 50 Å ± 10% respectively. T_m and J_{sc} of Cr cells are greater than those of Pd cells. FF is almost independent of properties of electrodes and varies with film properties and substrate. Mo substrates were used on cells 47 and 50. V_{oc} of Pd or Cr-N-I-P-Mo devices is almost the same as V_{oc} using a SS substrate, but FF using a Mo substrate is improved by 25-50%. A very heavily doped n-layer (10% of PH_3 in SiH_4) was used on cells 54 and 55. V_{oc} when using Cr on a

very heavily doped n-layer is almost the same as V_{oc} when using Cr on a less heavily doped n-layer (1% of PH_3 in SiH_4). V_{oc} when using Pd on a heavily doped n-layer is better than for a more lightly doped n-layer. This phenomena is similar to single crystalline silicon where heavily doped n-type materials form a good ohmic contact.[13] There was not a significant change of J_{sc} when using very heavily doped n-a-Si as a top layer. The variation of doping in the top Si layer by using 1%, 5% and 10% PH_3 in SiH_4 does not significantly change V_{oc}, J_{sc} and FF in Cr cells.

Variation of V_{oc} with top electrodes corresponds to semiconductor theory. The metallization process cannot assure an ohmic contact in a-Si:H solar cells since the heat treatment to make an alloy would cause dehydrogenation. The Schottky effect may occur in metal a-Si:H films due to a poor ohmic contact. An energy band diagram of N^+-I-P^+ metal solar cells is shown in Figure 9.

$$V_{bi_{eff}} = V_{bi} \text{ due to p-n junction} - V_{bi} \text{ due to metal - S.C} \quad (4\text{-}1)$$

$$V_{bi} \text{ due to metal - S.C} = q\,\phi_{Bp} - (E_F - E_V) \quad (4\text{-}2)$$

$$q\phi_{Bp} = E_g - q(\phi_m - x) \quad (4\text{-}3)$$

$$\text{then } V_{bi_{eff}} = V_{bi} \text{ due to p-n junction} - E_g + q(\phi_m - x) - (E_F - E_V) \quad (4\text{-}4)$$

where ϕ_m = work function of metal

x = electron affinity

E_g = energy bandgap of a-Si

As seen, $V_{bi_{eff}}$ increases with metal work function in N-I-P metal structures and decreases with work function in P-I-N metal structures.

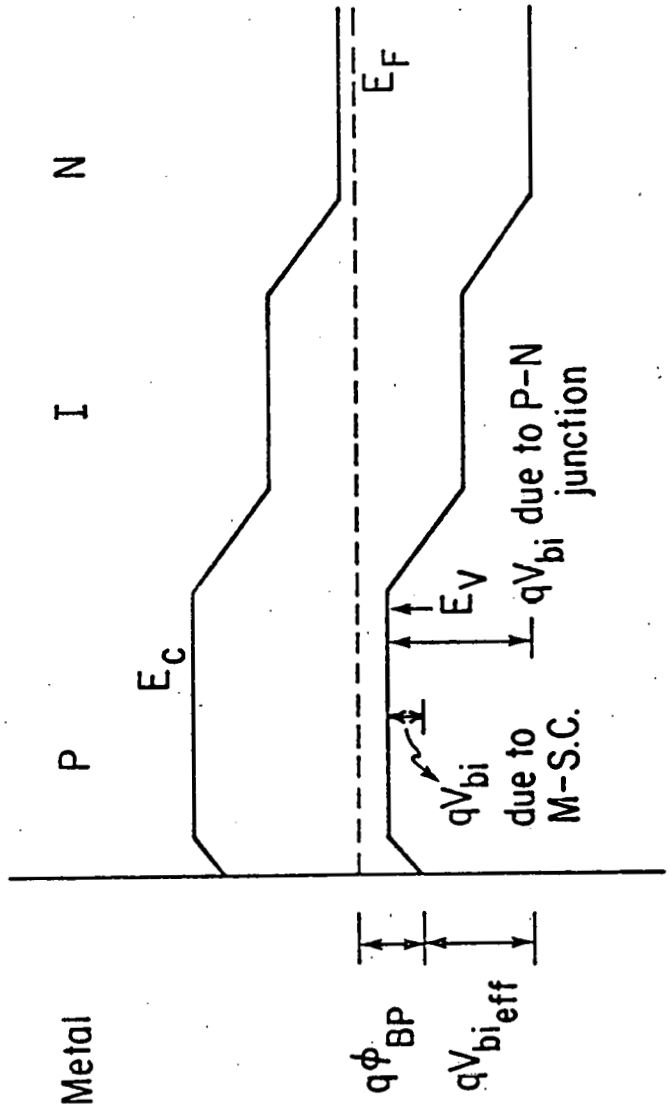

Figure 9. Energy Band Diagram for a P-I-N-Substrate Structure.

Solar generated current density is dependent on transmittance of top metal layers, absorption coefficient in the Si, width of the depletion region, and recombination centers. Internal current (I_{int}) defined by J_{sc}/T_m must be computed with great care since T_m and ρ_m vary greatly with thin film deposition conditions. J_{sc} of a cell with T_m = 64% and ρ_m = 800 Ω/[] is almost the same as J_{sc} of a cell with T_m = 35% and ρ_m = 18 Ω/[]. Fill factor is less dependent upon ρ_m since resistivity of the a-Si:H film and contact resistance between substrate and film are very large. Reduction of effective collection width due to the forward bias may be responsible for a low fill factor.

5. I-V CHARACTERISTICS OF a-Si:H SOLAR CELL

5-1 Dark I-V Characteristics

Dark I-V characteristics are used to evaluate conduction processes in diodes. Figure 10 shows typical dark I-V characteristics of a-Si:H solar cells to compare Schottky barrier, P-I-N and N-I-P structures. Although superposition of short circuit current into dark I-V characteristics does not describe photovoltaic behavior since photogenerated current is strongly dependent on the depletion region, the V_{oc} is strongly related to the reverse saturation current (J_o) and diode quality factor (n). V_{oc} of SB, P-I-N and N-I-P solar cells is typically 475 mV, 540 mV and 700 mV respectively. Higher J_o and low V_{oc} was expected in the SB cell since the Schottky metal was Pd. Film properties of N-I-P and P-I-N structures are almost identical but dark I-V characteristics are quite different. This illustrates the difficulty in interpreting J_o and n values only in terms of the volume properties of devices. Although the results indicate that the current is limited by recombination in the junction region, as in crystalline Si diodes, other factors involving the substrate and electrode play significant roles in determining the characteristics of a-Si:H devices.

Figure 11 shows a dark J-V characteristic for a typical a-Si:H solar cell with a N-I-P-SS structure which always produces better performance than P-I-N and SB structures. Shunt resistance and recombination mechanisms dominate in the low forward bias regime. Series resistance plays an important role in the far forward bias region. Between these extremes (0.3 $\sim$ 0.7 V), the diode quality factor n lies between 2.3 $\sim$ 2.7. The saturation current density (J_o) is around 10^{-8} to 10^{-9} A/cm^2. The n-factor for poor quality solar cells is greater than 3.0 and sometimes greater than 5.0. Accurate analysis of the deviation of the ideality factor from 1 and the relation

FIGURE 10. Dark I-V Characteristics of a-Si:H Solar Cells

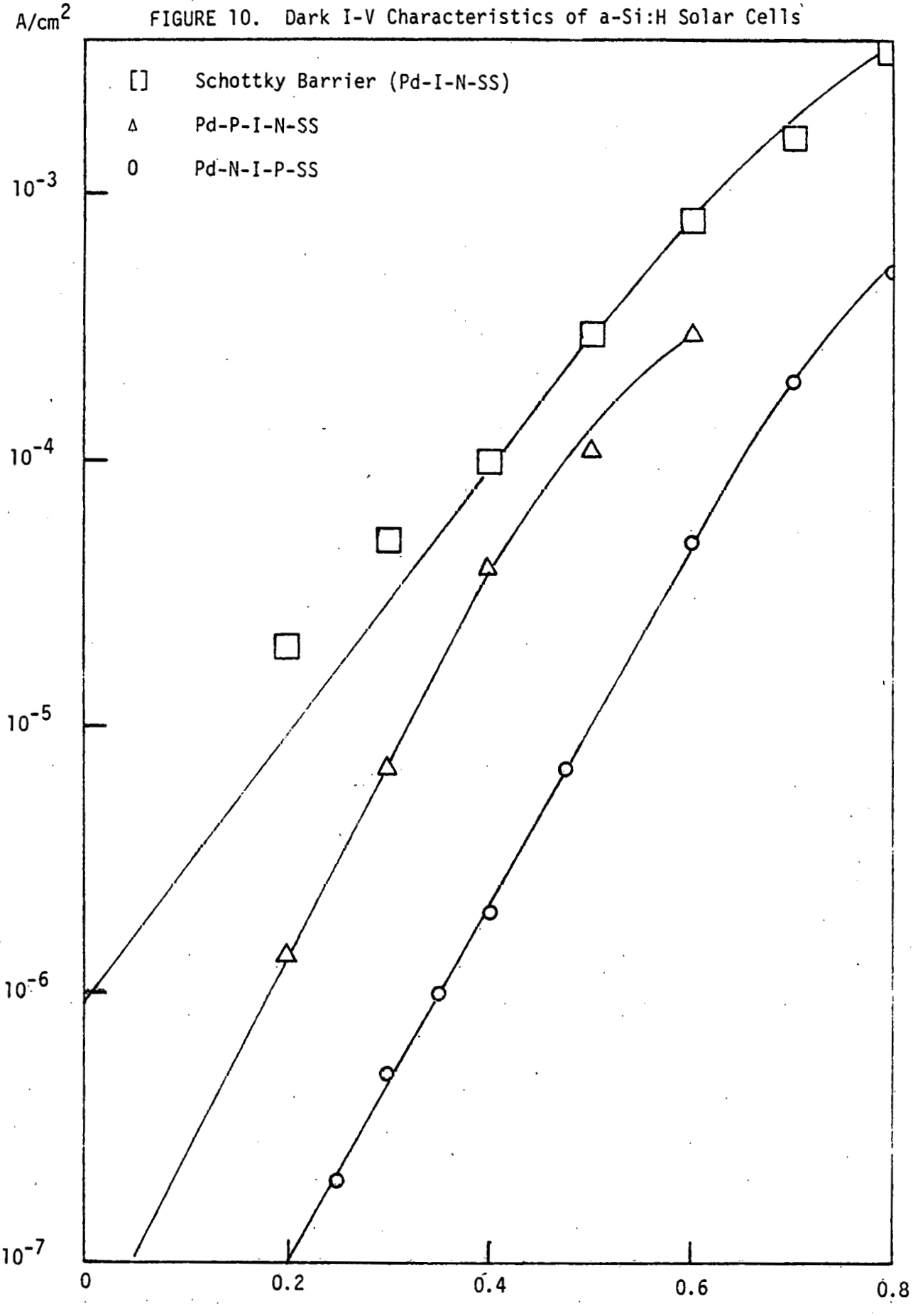

Figure 11. Typical Dark J-V Characteristics of a-Si:H Cell with a N-I-P structure

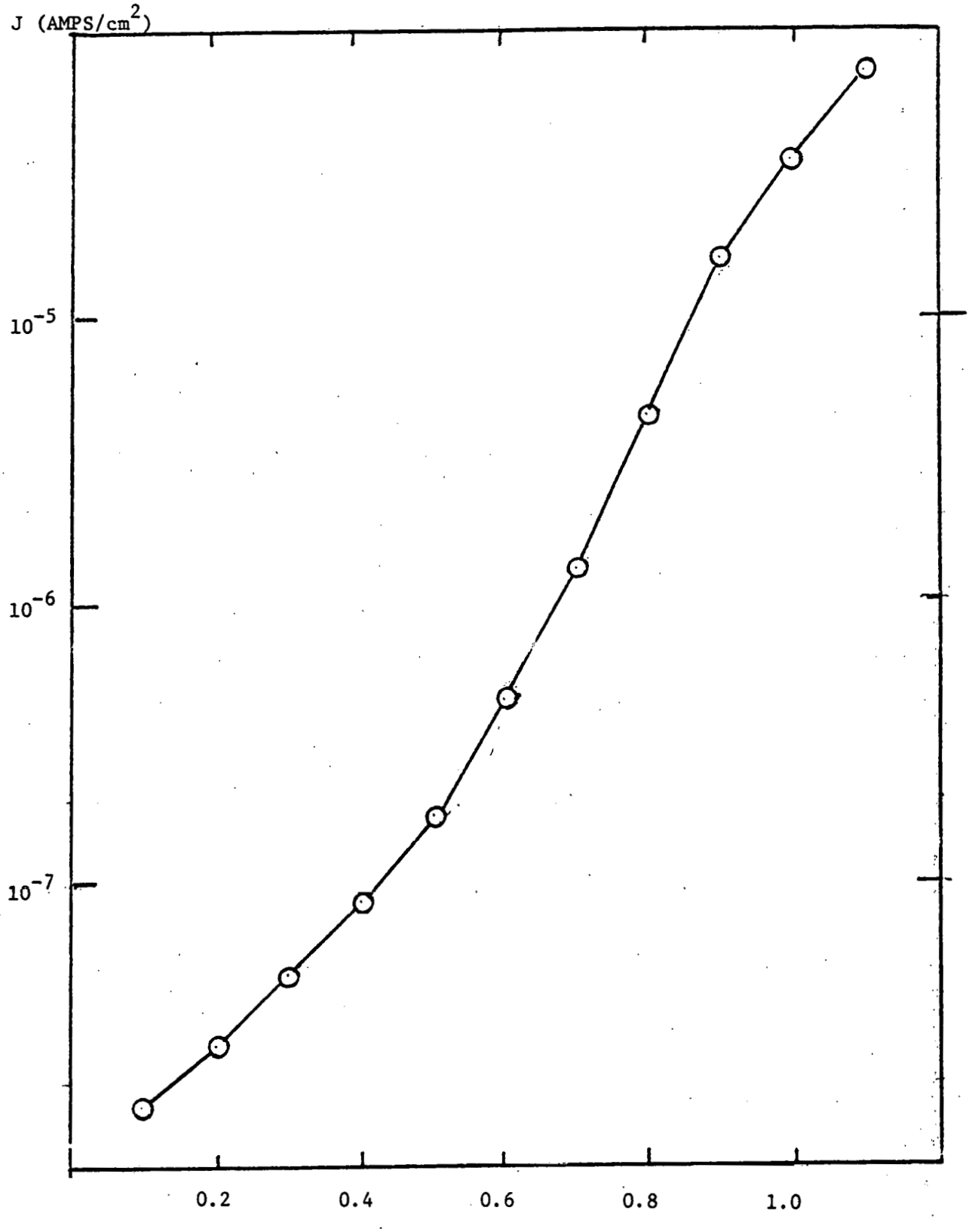

between quality of film and n value is not well known but probably is due in part to the leakage current caused by shunt resistance and recombination mechanisms in the depletion region.

Dark J-V characteristics of different diodes on the same substrate in Figure 12 show shunt resistance, saturation current and ideality factor to depend upon uniformity and quality of the film. Three different characteristics are obtained from three diodes on the same substrate. There are serious differences in the low forward bias regime of diodes L4 and R5 due to shunt resistance but this difference is reduced near the open circuit voltage region. It appears that cell R5 of sample 15-29 is better than cell L4. But, V_{oc} of L4 was 780 mV and that of R5 was 760 mV while FF and J_{sc} were the same. These differences do not appear in all cases and have been largely eliminated in some of the more recent substrates.

Uniformity of a-Si films has been improved with film thickness. Dark J-V characteristics of different cells from the same sample (an improved substrate) are identical in Figure 13. The probability of defects or pinholes due to roughness of the substrate can be reduced with thicker films. Thickness of Si could greatly change the series resistance of a-Si:H cells. R_s is determined by the quasi-neutral region and is given by $R_s = (L-W_B)/\sigma$, where σ is the conductivity of the a-Si:H. W_B, determined from spectral analysis by considering only the drift mechanism, is $0.2 \sim 0.4$ μm in a-Si:H cells under illumination. In single crystalline or polycrystalline cells, $L >> W_B$ and R_s increases linearly with thickness L. In a-Si:H cells, $L >> W_B$ does not hold and R_s may increase much more with thickness.

FIGURE 12

DARK J-V OF DIFFERENT DIODES FROM THE SAME SUBSTRATE (#15-29)
(CR-N^+-I-P^+-SS)

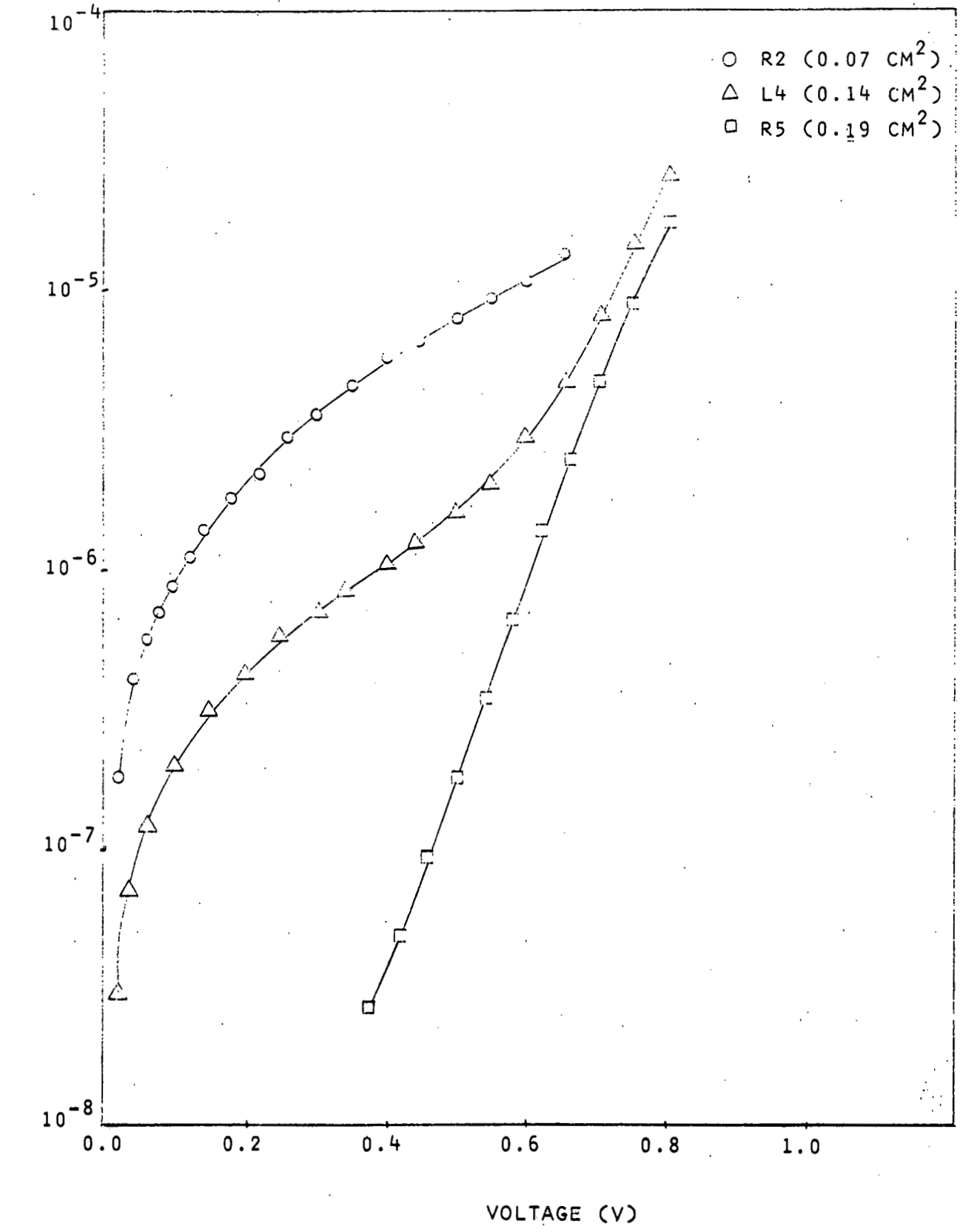

FIGURE 13

DARK J-V OF DIFFERENT DIODES FROM THE SAME SUBSTRATE (#20-93)

(CR-N^+-I-P^+SS)

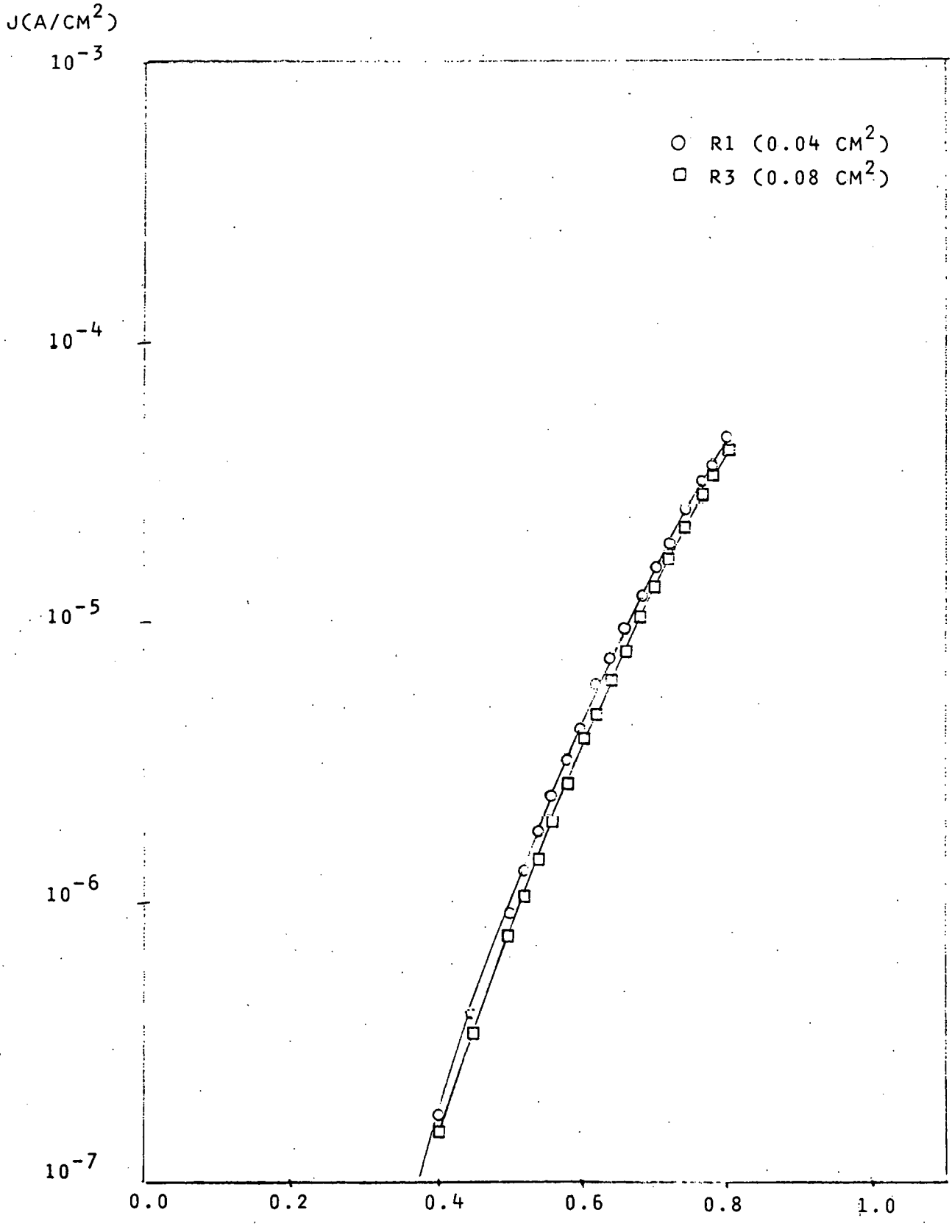

Our experimental results suggest that dark current characteristics do not always play a significant role in determining illumination characteristics in a-Si:H cells. Figure 14, shows the almost identical dark I-V data for Cr and Pd cells on the same substrate (N-I-P-SS) while illuminated characteristics are quite different. It is quite likely that current conduction mechanisms under dark conditions are different from those during illumination. Differences of n values (2-5) for dark characteristics and n_ℓ (1.5) during illumination also suggest that recombination mechanisms may be quite different.

FIGURE 14
DARK J-V OF CR-N^+-I-P^+/SS AND PD-N^+I-P^+/SS CELLS ON THE SAME SUBSTRATE

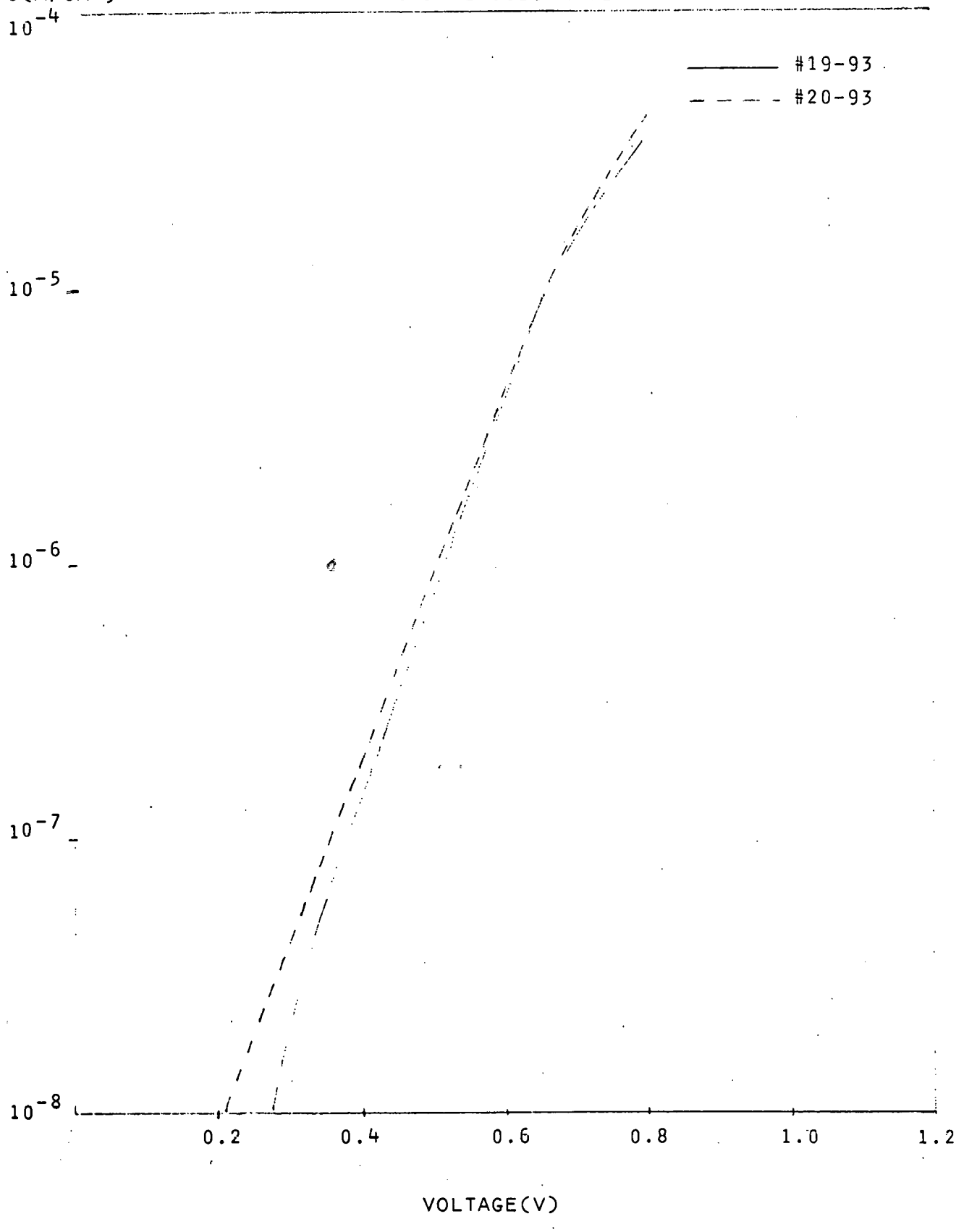

5-2 Illuminated Characteristics

Typical illuminated characteristics are shown in Figure 15 for two P-N junction type cells. Two important phenomena can be seen; photogenerated current is not saturated in the reverse region and the superposition principle does not apply. Photogenerated current J_L is very much dependent upon the depletion region width. This dependence is shown by

$$J_L(V) = F\,(1-\exp(-\alpha W_B(V)) + \text{diffusion term} \qquad (5\text{-}1)$$

$$W_B(V) = (V_o - V)^{\frac{1}{2}}\, f(N) \qquad (5\text{-}2)$$

where F = total incident photon flux

W_B = depletion width at V

V_o = built-in-potential

f(N) = function of space charge density N.

Short circuit current density (J_{sc}) increases almost linearily with illumination level as shown in Figure 16. Although this result agrees with previously reported results,[7,14] it contradicts our spectral response results. From the spectral response analysis under different illumination levels, spectral response under weak illumination is 30-100% larger than under AM1 illumination. Short circuit current should not increase linearily with illumination level. One of the reasons for an apparent linear relationship between J_{sc} and illumination level is that the ELH lamp is used for the simulation of AM1 illumination. The spectral density of an ELH lamp does not vary linearily with illumination level. The visible spectrum of an ELH lamp decreases more than linearily while the IR spectrum of an ELH lamp decreases by a lesser amount. Figure 17 shows the normalized spectral density of the ELH lamp. To verify J_{sc} vs

FIGURE 15

ILLUMINATED I-V CURVES

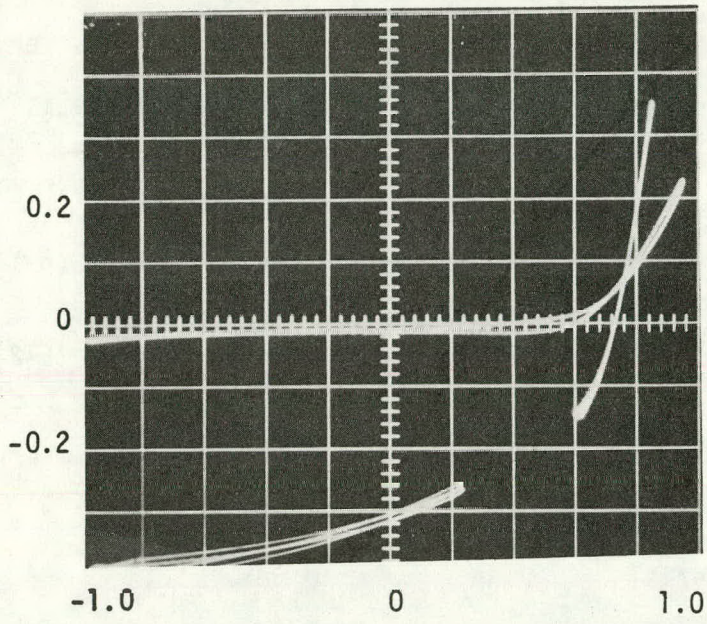

#21-85
Cr-N-I-P-SS
Area = 0.13 cm^2
(30% Shadowed)

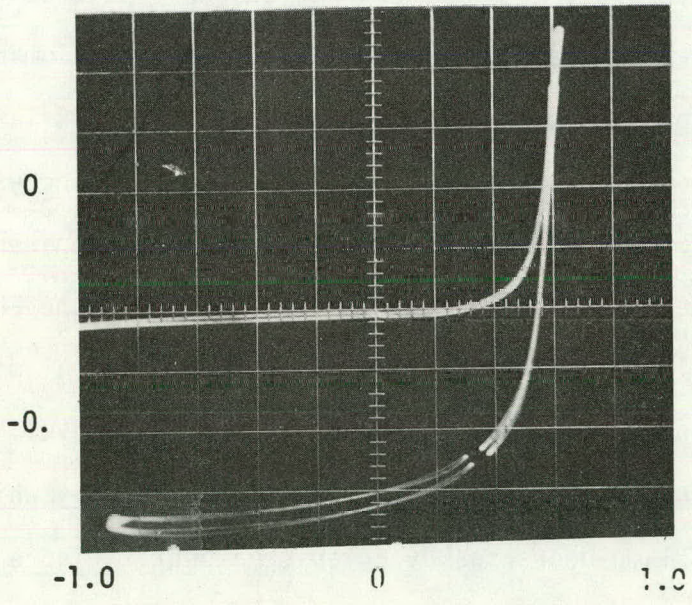

#8-30
Pd-P-I-N-SS
Area = 0.11 cm^2
(50% Shadowed)

FIGURE 16

I_{SC} VS INTENSITY (CELL #20-93)

(CR-N^+-I-P^+-SS)

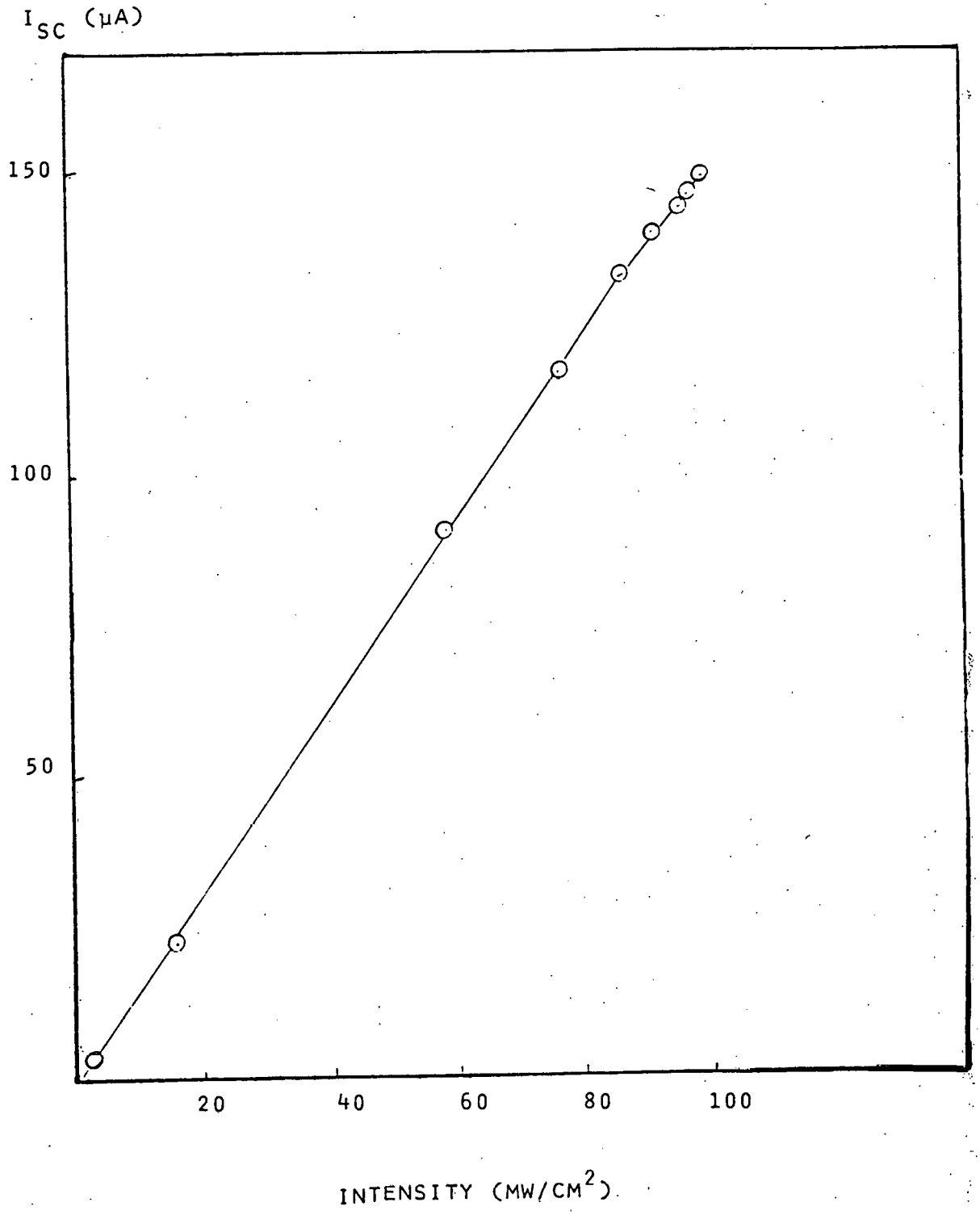

FIGURE 17. NORMALIZED SPECTRAL DENISTY OF AN ELH LAMP

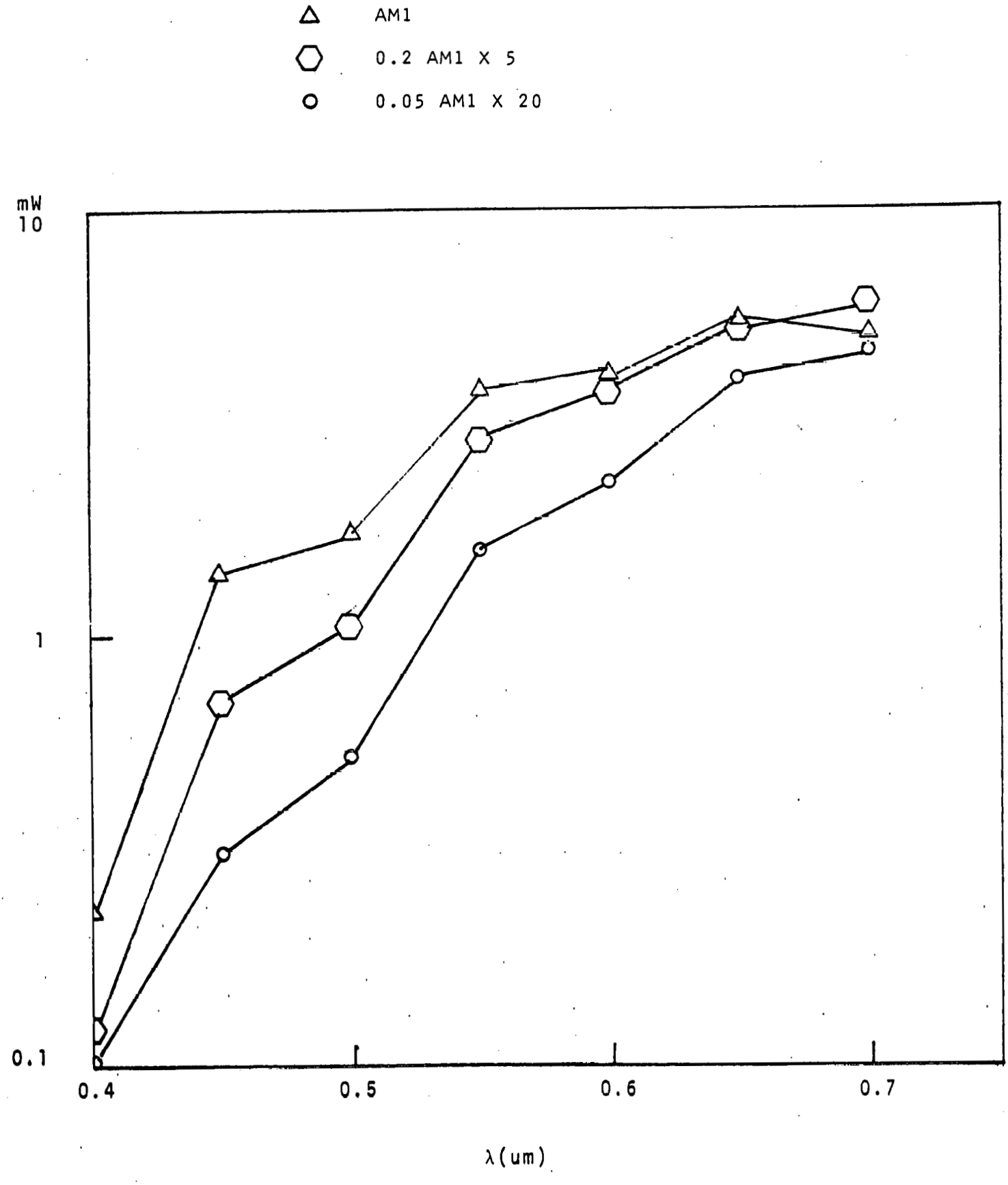

V_{oc}, there must be extreme care concerning the spectral distribution of the lamp. A neutral density filter will be ideal for this experiment. Although the superposition principal does not hold, the open circuit voltage under illumination can be expressed as

$$V_{oc} = \frac{n_\ell \cdot kT}{q} \ln \left(\frac{J_{sc}}{J_{oL}} + 1\right) \qquad (5\text{-}3)$$

where n_ℓ = diode factor under illumination

J_{oL} = saturation current under illumination

n_ℓ is around 1.5 and J_{oL} is around 10^{-10} to 10^{-12} A/cm^2 from analysis of data in Figure 18. These values are much less than the corresponding parameters of the dark J-V characteristics where J_o is around 10^{-9} A/cm^2 and n is around 2.5. The J-V characteristics for a-Si:H solar cells are greatly improved under illumination as far as low ideality factor and low saturation current are concerned. These effects are related to photoconductivity of a-Si:H during illumination. The trapping of photogenerated holes may cause the undoped layer to behave like an n-type material. It is well known that the drift mobility of holes and electrons in a-Si:H is trap controlled with $\mu_e >> \mu_h$. This effect can lead to $n_\ell < n$ and $J_{oL} < J_o$.

I-V characteristics for different illumination levels is shown in Figure 19. Low shunt resistance influences the fill factor of a-Si:H cells as evidenced by the fact that FF with 0.01 AM1 illumination is lower than FF with AM1 illumination. This phenomena has almost disappeared in the more recent cells due to the improvement of film uniformity and quality.

Figure 18. J_{sc} vs V_{oc} and Dark J-V

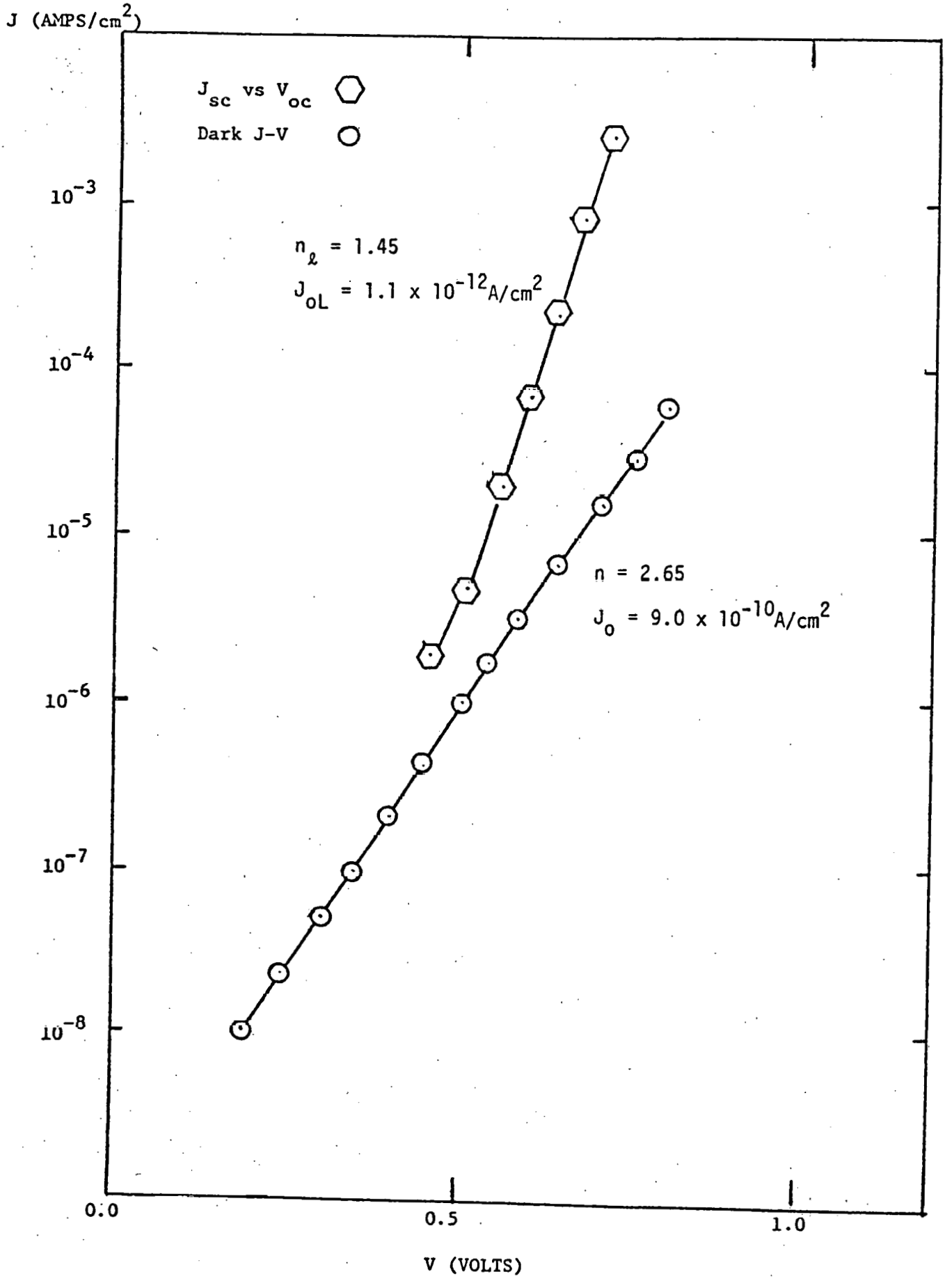

FIGURE 19

I-V CHARACTERISTICS UNDER DIFFERENT ILLUMINATION LEVELS

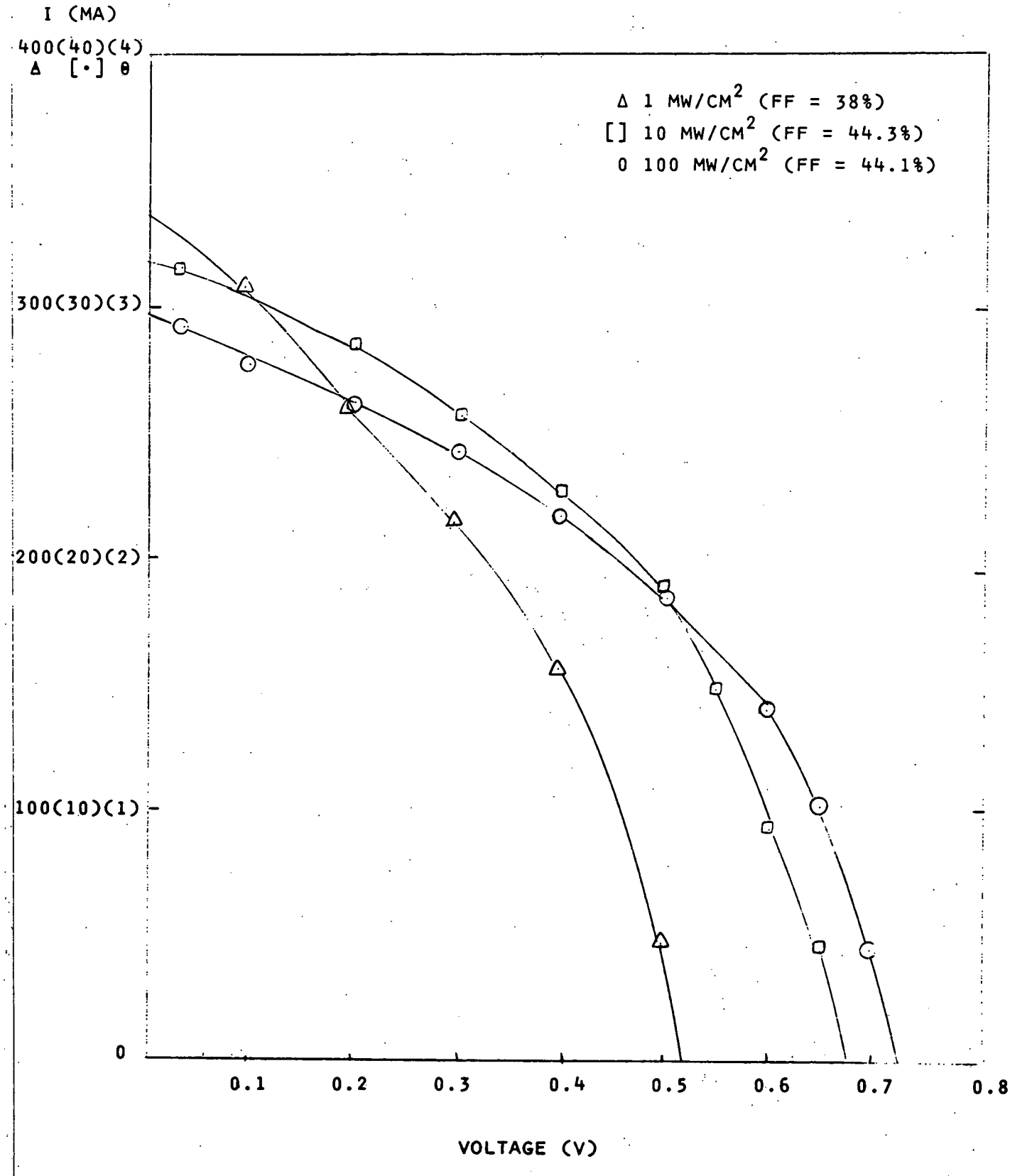

6. CARRIER COLLECTION AND RECOMBINATION

6-1 A Model for Collection Mechanisms

The important parameters, such as J_{sc}, V_{oc} and FF, which determine the photovoltaic performance of solar cells, depend on the generation and recombination mechanisms of photoexcited carriers. Hole diffusion length (L_p) of undoped a-Si:H is extremely small (less than 350 Å has been reported),[15] so that we can normally neglect the diffusion contribution of photoexcited carriers to the generation mechanisms. Then the importance of a field assisted drift process of photoexcited carriers is realized in low diffusion length materials. In a-Si:H solar cells, we assume that all the photogeneration takes place in the depletion region where a strong field exists.

In the recombination mechanisms of a-Si:H, volume recombination or geminate recombination can be considered depending on the rate of diffusion of photoexcited carriers. The mean free path of photoexcited carriers is very small in a low mobility material like a-Si:H so that recombination is controlled by the rate of diffusion of excited carriers. Geminite recombination[16] has been considered to be the dominant recombination mechanism in a-Si:H. If geminite recombination is indeed dominant, it would be a serious limitation for the development of efficient solar cells.

To investigate generation and recombination in semiconductor material, we choose to use spectral response analysis to measure collection efficiency. In order to compare collection efficiency of different solar cells, it is necessary to eliminate effects due to variations in the optical transmittance of the semitransparent metal electrode. Transmit-

tance of the top electrode is varied with the thickness of metal film and deposition rate. As outlined in Chapter 3, to avoid this problem, transmittance and resistivity of each thin metal film was measured after solar cell fabrication. Then we can utilize the internal collection efficiency

$$QE_i\ (\lambda) = QE_e\ (\lambda)/T\ (\lambda) \qquad (6\text{-}1)$$

where QE_i = internal collection efficiency

QE_i = external collection efficiency

T = transmittance of the top electrode

The collection efficiency is related to the spectral response by the expression

$$QE\ (\lambda) = SR\ (\lambda)\ E\ (\lambda) \qquad (6\text{-}2)$$

where SR = spectral response

$E\ (\lambda) = hc/\lambda$

The spectral response characteristics were increased using a calbriated NASA Lewis standard p-n junction cell. An Oriel narrow hand filter set with band widths between 5-10 nm and a Schoeffel GM 100 10 grating monochrometer in conjunction with an ELH quartz-halogen lamp source were used to provide a spectral range of 400 - 950 nm. The dispersion in the monochrometer was less than 8.5 nm. The absolute spectral response (mA/mW) of the test cell, SR (λ) was calculated using

$$SR\ (\lambda) = \frac{\text{Test cell current density}}{\text{Reference cell current density}}\ X\ (SR\ (\lambda))_{std} \qquad (6\text{-}3)$$

In order to develop a carrier collection model, we considered the fraction of photogenerated carriers which actually contribute to current.

If N_o is the photon flux density entering the semiconductor at wavelength λ, then the flux of minority carrier entering the Schottky metal contact is

$$F = N_o [1 - \exp(-\alpha W)] + N_o \exp(-\alpha W) \frac{\alpha L_n}{1 + \alpha L_n} \qquad (6\text{-}4)$$

The diffusion length (L_n) is less than 0.1 μm and α is less than 10^6/cm. W, depletion region width, is of the order of a few tenths of a micron. In the short wavelength region, αL_n is not << 1, but $\exp(-\alpha W)$ is very small. In the long wavelength region, αL_n << 1 so that the $\frac{\alpha L_n}{1 + \alpha L_n}$ term can be neglected. Then equation 6-4 can be reduced to

$$F = N_o [1 - \exp(-\alpha W)] . \qquad (6\text{-}5)$$

In this approximation we do not consider the effects of surface imperfections, reflection at the back surface, or field contribution between the I-N region near the substrate.

If drift distance is smaller than the depletion region width then carriers will be recombined in the depletion region. Drift distance (L_D) can be defined as

$$L_D = \mu\tau E . \qquad (6\text{-}6)$$

where μ = mobility

τ = carrier lifetime

E = electric field

Then we take into account the drift distance in equation 6-5 to give

$$F = N_o [1 - \exp[-W(\alpha + \frac{1}{L_D})]] \times \frac{\alpha L_D}{1 + \alpha L_D} \qquad (6\text{-}7)$$

Diffusion length of holes of undoped a-Si:H is less than 0.1 nm. Using the Einstein relation $\mu kT = qD$ and the expression for diffusion length $L = \sqrt{D\tau}$, we can calculate $\mu\tau$ directly from the diffusion length. $\mu\tau$ is of the order of 10^{-8} to 10^{-9} cm^2/V. For a depletion region width of a few tenths of a micron, the average value of field is greater than 5×10^4 V/cm. Then drift distance $L_D = \mu\tau E$ is greater than the depletion

region and $1/L_D << \alpha$ even in the long wavelength region.

In a-Si:H cells, the drift distance of carriers in the depletion region is not a serious limitation of carrier collection efficiency. As illustrated, the depletion region width is the most important factor to determine carrier collection. In an ideal Schottky barrier cell, the depletion region is expressed by

$$W = \left(\frac{2q\varepsilon_s V}{N_s}\right)^{\frac{1}{2}} \qquad (6\text{-}8)$$

where V = voltage drop across $W = (V_{bi} - V - \frac{kT}{q})$

N_s = space charge density

ε_s = dielectric constant.

In contrast with a single crystalline cell, N_s in a-Si depends on the illumination. V depends on the Schottky metal and applied bias. N_s can depend on the incident photon flux since holes and electrons are not trapped in equal numbers. More holes than electrons are trapped and N_s increases with increasing light intensity. To measure N_s and depletion width, capacitance C as a function of applied bias can be utilized. We utilize a collection efficiency model based upon equation 6-5.

In P-I-N or N-I-P type cells the collection mechanism is not well established as in Schottky barrier cells. From the classical paper of Carlson,[6] the best photovoltaic data are obtained by illuminating the p-side. Therefore, it is established that carrier collection in P-N junction types of a-Si:H cells exists near the depletion region between P-I rather than I-N. These assumptions seem very attractive since the undoped layer behaves as n-type under illumination due to the hole trapping effect.

This phenomena leads to the assumption that in N-I-P cells, the major collection of carriers takes place in the depletion region between I-P rather than N-I near the illuminating side. To investigate the principal carrier collection region in N-I-P- substrate structures, we have changed the thickness of the undoped layer from 0.5 μm to 1.0 μm. There is not a significant difference in J_{sc} between a 0.5 μm and 1.0 μm I-layer cell. These results indicate that the principle current collection region is not the depletion region due to the P-I layer in N-I-P cells but due to the depletion region of the N-I layer. These results suggest that fundamental current collection mechanisms of N-I-P and P-I-N cells are basically the same as those in a Schottky barrier. Principal current collection takes place near the surface regardless of the cell structure.

The difference between P-N junction types and Schottky barrier structure lies in the fact that there exists a dead layer near the top of the p-n type cell where absorbed carriers cannot be utilized. This dead layer concept is very similar to that found in single crystalline cells.[4] In the heavily doped layer, diffusion length is small and absorbed carriers in the doped layer must rely on drift mechanisms. The depletion region in the doped layer also is very small compared with depletion region in the undoped layer.

We divide the carrier collection area in the P-N junction a-Si:H cells into two regions, carrier collection from the top layer and carrier collection from the undoped layer as shown in Figure 20. Although W_D is much smaller than W_I due to the fact that N_{SD} is much larger the N_{SI}, the spectral response in the ultraviolet regime is controlled by W_D since absorption is very strong.

Total collection efficiency, N_T is given by $N_D + N_I$.

where N_D = collection from the doped region

N_I = collection from the undoped region.

$$N_D(\lambda) = \exp[-\alpha_D(\lambda)X_j] - \exp[-\alpha_D(\lambda)(X_j-W_D)] \qquad (6\text{-}9)$$

$$N_I(\lambda) = \exp[-\alpha_D(\lambda)X_j][1 - \exp(-\alpha(\lambda)W_I)] \qquad (6\text{-}10)$$

where X_j = junction depth

W_D = collection width in the doped layer

W_I = collection width in the undoped layer

$\alpha_D(\lambda)$ = absorption coefficient of the doped layer

$\alpha(\lambda)$ = absorption coefficient of the undoped layer

The absorption coefficient of the undoped layer was measured as outlined in Chapter 2 but absorption coefficient of the doped layer has not yet been well established. We thus assume $\alpha_D(\lambda) = K\,\alpha(\lambda)$ with $1 < K < 2$.

In the short wavelength region, the N_D term is dominant since $\alpha(\lambda)$ at short wavelength is very large and most of the incident photons are absorbed within a few hundred anggtroms. In the long wavelength region, the N_I term is dominant since $\alpha(\lambda)$ at long wavelength is small enough so that a very small fraction of incident photons is absorbed within the doped region in a thickness less than a few hundred anggtroms. Dead layer thickness (X_j-W_D) can be calculated from equation 6-9 by subtracting short wavelength collection efficiency from unity. Collection region W_I can be calculated from equation 6-10 by utilizing the long wavelength collection efficiency. A comparison between the computer model and experimental data is given in the next section.

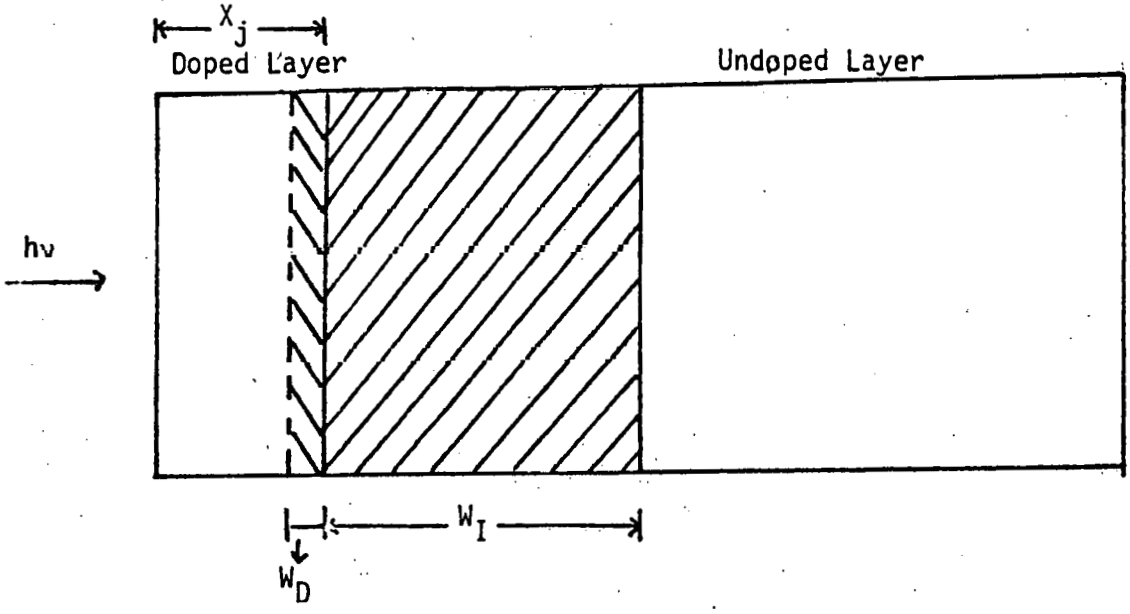

Figure 20. Carrier Collection Regions.

6-2 Experimental Results and Discussion

Figure 21 shows the typical collection efficiency calculated from spectral response measurements. In Schottky barrier cells, we notice the loss of collection efficiency in the ultraviolet region possibly due to a Schottky barrier lowering effect. In an ideal Schottky barrier, Schottky barrier lowering due to image force effects can cause a field having a direction opposite to the Schottky field. We wish to discuss this theory as one explanation for our experimental data.

From basic image force theory, there exists a distance X_m from the Schottky barrier metal within the semiconductor causing the surface electric field to be modified such that both photoexcited carriers eventually recombine and thus do not contribute to photocurrent. The location of this lowering (X_m) is given by[13]

$$X_m = \left(\frac{q}{16\ \pi\ \varepsilon_o E}\right)^{\frac{1}{2}} \text{ cm} . \qquad (6\text{-}11)$$

where E = electric field.

ε_o = permittivity of free space

X_m is about 60 Å for E = 10^5 V/cm and 10 Å for E = 10^7 V/cm. In a-Si:H, the electric field is around $10^4 \sim 10^5$ V/cm and X_m can be around 30 Å $\sim$ 60 Å. The region between the surface and X_m behaves like a dead layer or reverse biased junction. 15% and 25% of incident photons of ultraviolet will be absorbed within 30 Å and 60 Å where α is 4×10^5 cm^{-1} and may then be lost.

X_m varies inversely with space charge density so that the image force effect may be a serious limitation under weak illumination. Figure 22, shows the collection efficiency of a Schottky barrier under different illumination levels. Collection efficiency in the IR region is increased

Figure 21. Collection Efficiency of Schottky Barrier, N-I-P and P-I-N a-Si:H Cells

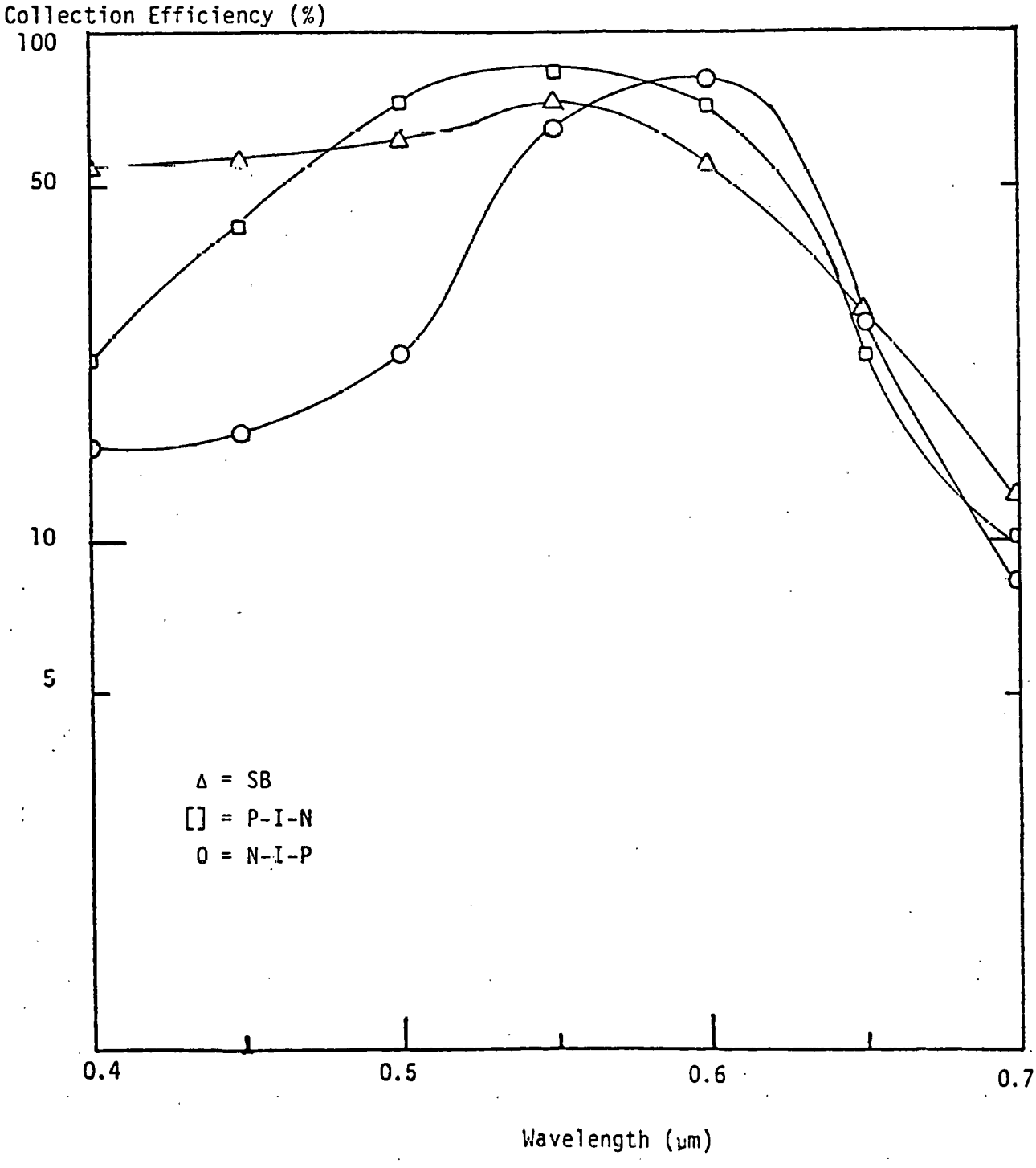

Figure 22. Collection Efficiency Variation with Illumination Level for Schottky Cells.

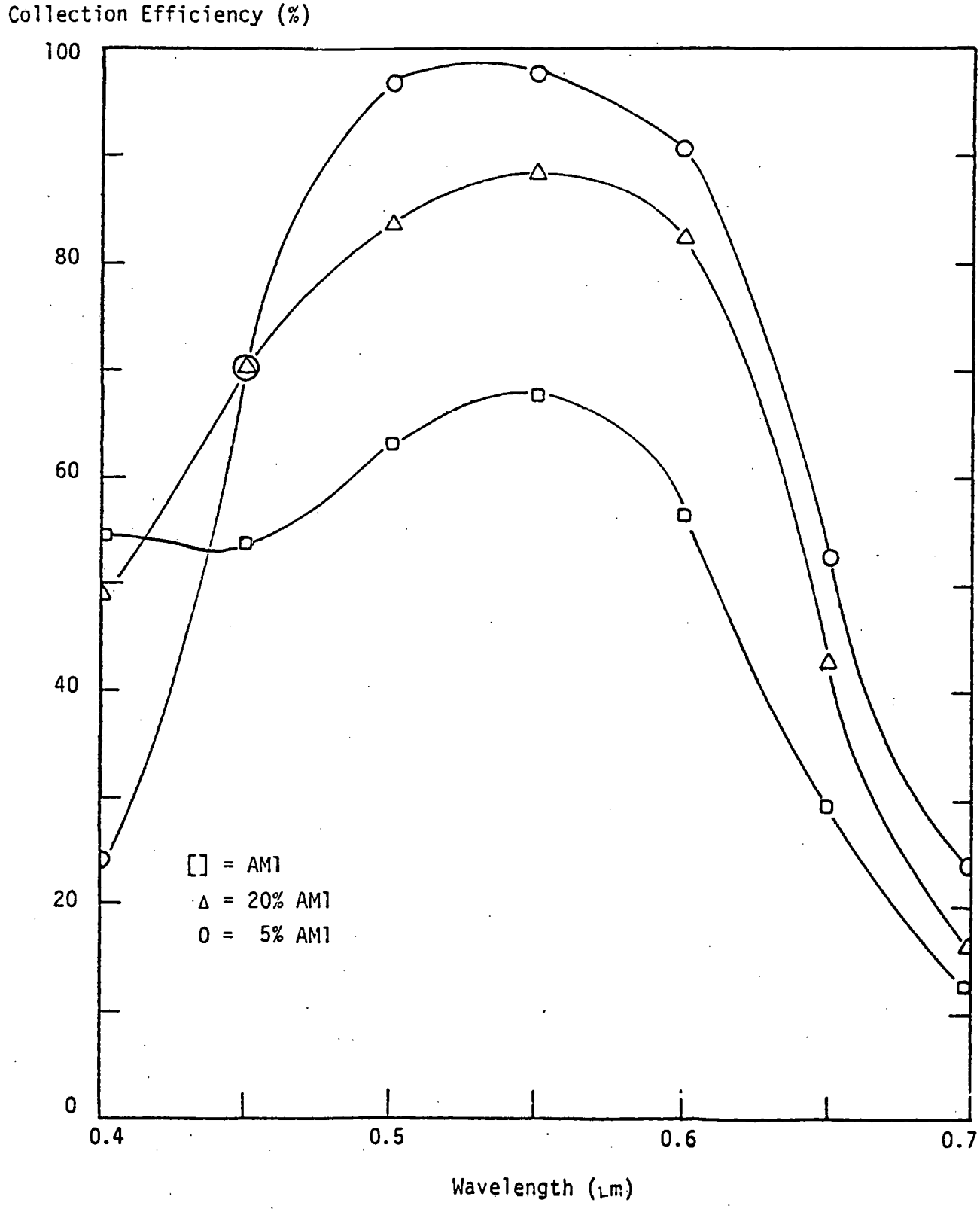

with weak illumination due to the decrease of space charge density N_s while UV response is decreased due possibly to image force lowering. This phenomena was previously reported without explanation.[17]

In P-I-N or N-I-P type cells, collection efficiency is similar to that for Schottky type cells except for poor UV response due to absorption in the doped layer. Peak collection efficiency of P-I-N and N-I-P cells occurs at 0.55 μm and 0.6 μm, respectively. The shift of peak response is due to thickness of the top doped layer. The top doped layer for P-I-N and N-I-P cells are 100-200 Å and 300-450 Å. Thus, in N-I-P cells, strong absorption occurs in the short wavelength region but these surface generated carriers are not collected. To verify the collection region of N-I-P type cells, we measure the dependence of monochromatic photocurrent $J_L(V)$/short circuit photocurrent ($J_L(0)$) ratio for several wavelengths. $J_L(V)/J_L(0)$ for reverse bias clearly shows the location of the principal collection region to be between N-I rather than I-P. This is evidenced by decreased voltage sensitivity at λ = 0.6 μm and λ = 0.7 μm in Figure 23. UV response increases rapidly with reverse bias since the dead layer width is decreased due to the increase of W_D.

In P-N type a-Si:H cells, the image force lowering effect is not serious since the top layer is heavily doped and the electric field between semitransparent thin metal film and a-Si:H is very small compared with a Schottky barrier cell. As seen in Figure 21, collection efficiency in the ultraviolet regime is poor due to the absorption in the doped surface layer. Figure 24 shows the collection efficiency of a P-I-N type cell under different illumination levels. Collection efficiency increases with decrease in illumination due to expansion of the depletion region caused by a decrease in N_s. In the ultraviolet regime, due to the image force effect, we can see a slight decrease in collection efficiency.

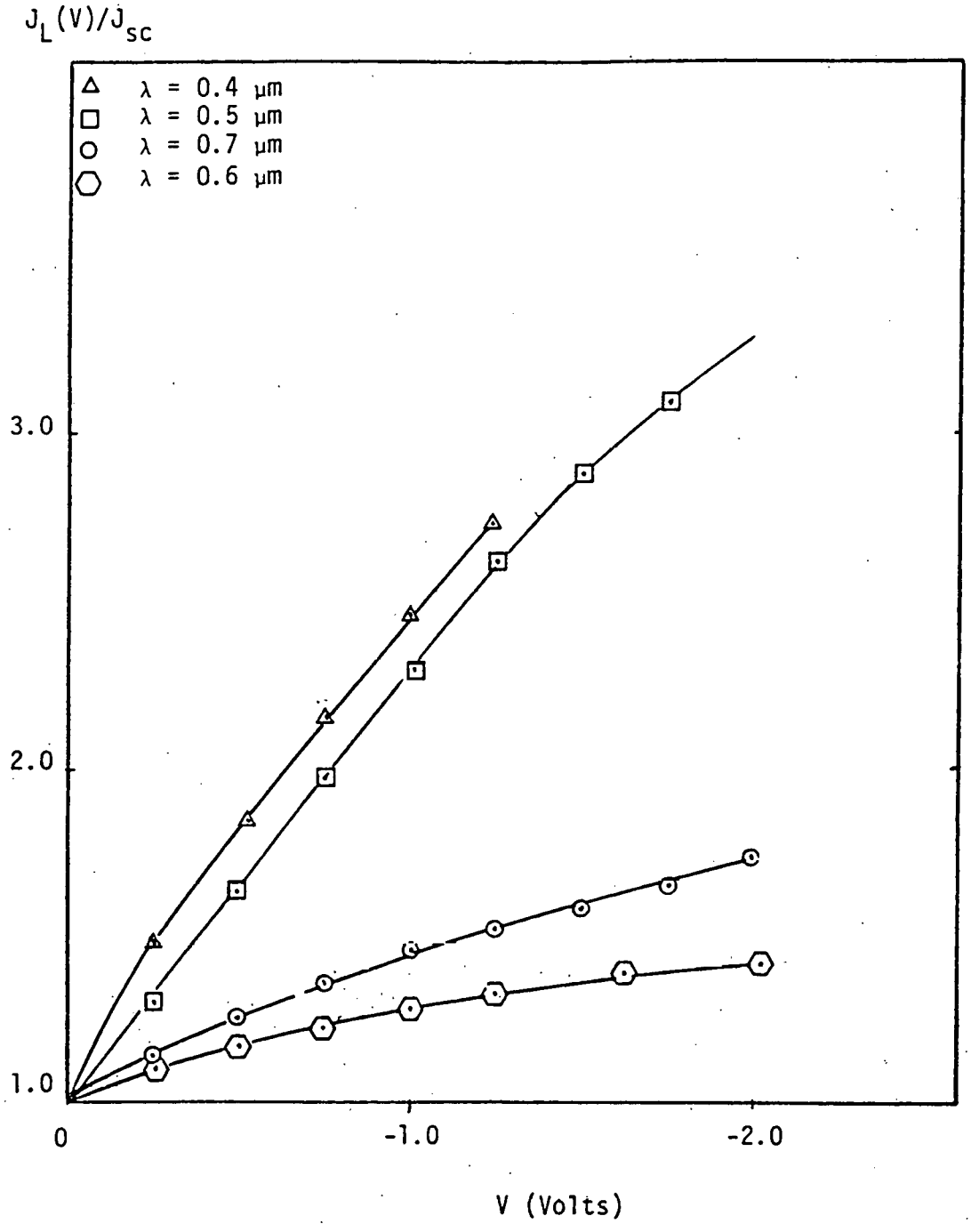

Figure 23. The ratio of monochromatic photocurrents J to J_{sc} as a function of reverse bias.

Figure 24. Collection Efficiency Variation with Illumination Level for a P-I-N Cell.

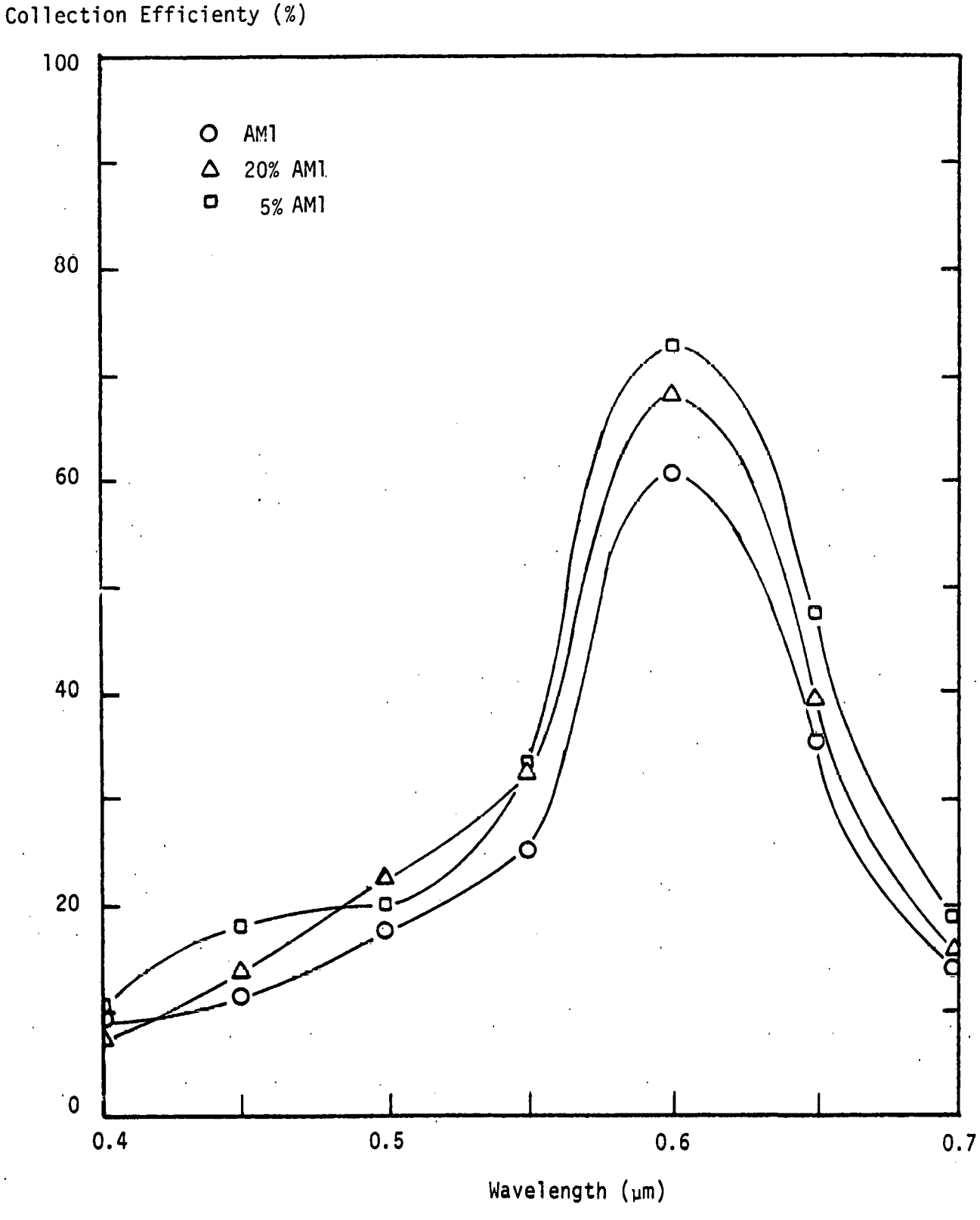

We can see in both Schottky and P-N junction type cells, under weak illumination, that collection efficiency is near unity. This suggests that geminite recombination is not a serious limitation in our cells. To improve collection efficiency of P-N type cells, we must decrease the dead layer width. We have developed a computer model to relate dead layer width and J_{sc} which uses the basic equation

$$J_{sc} = q \int F(\lambda)\, N_T(\lambda)\, dX \qquad (6\text{-}12)$$

$F(\lambda)$ was obtained from a table of the standard AM1 spectrum from Takehara.[18] Figure 25 shows that J_{sc} is increased substantially with a decrease in width of this dead layer.

We have thus discussed the importance of thickness of the top doped layer in N-I-P and P-I-N cells. Also, we propose that Schottky barrier lowering can decrease UV response in M-S cells. Surface state effects could also decrease the UV response as well.

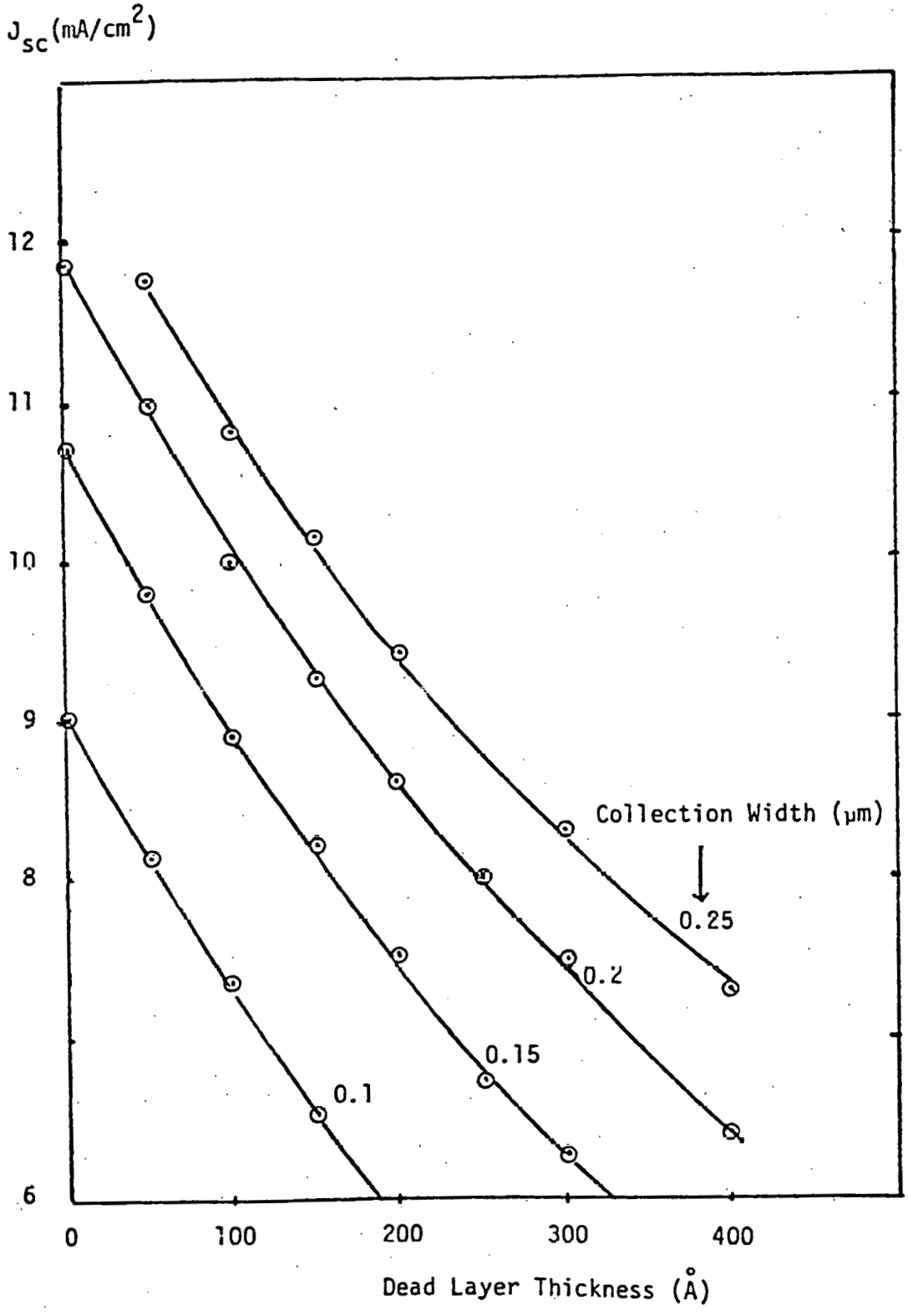

Figure 25. Short Circuit current Density as a function of Collection Width and Dead Layer

7. REFERENCES

1. M. H. Brodsky, Amorphous Semiconductors, Springer-Verlag, Berlin, 1979.

2. D. E. Carlson, Photovoltaic Advanced R & D Annual Review Meeting Denver Colorado, September 1979.

3. C. R. Wronski, D. E. Carlson, R. E. Daniel and A. R. Triano, 1976 International Electron Device Meeting, Washington, D.C. December 1976.

4. H. J. Hovel, Solar Cells, Academic Press, New York, 1975.

5. W. A. Anderson, S. M. Vernon, A. E. Delahoy, J. Kim and P. Mathe, J. Vac. Sci. Tech., 13, No. 6, 1976.

6. D. E. Carlson, IEEE Trans. Elec. Dev., ED-24, No. 4, 1977.

7. W. A. Anderson, J. Kim, S. Hyland, J. Coleman and T. Woo, 13th IEEE Photovoltaic Specialist Conference, Washington, D.C., June 1978.

8. J. Stone, Photovoltaic Advanced R & D Annual Review Meeting, Denver, Colorado, September 1979.

9. R. A. Gibson, W. E. Spear, P. G. LeComber and A. J. Snell, J. of Noncrystalline Solids, Vol. 35 and 36, 1980.

10. D. E. Carlson, a-Si Review Meeting, April 23-25, 1980, Washington, D.C.

11. V. L. Dalal, IEEE Trans. Elec. Dev., ED-27, No. 4, 1980.

12. D. E. Carlson, C. R. Wronski, J. Electron Material, Vol. 6, 1977.

13. S. M. Sze, Physics of Semiconductor Devices, Wiley, New York, 1969.

14. C. R. Wronski, IEEE Trans. Elec. Dev., ED-24, No. 4, 1977.

15. D. L. Staebler, J. of Noncrystalline Solids, Vol. 35 and 36, 1980.

16. L. Onsager, Phys. Rev., 54, 554 (1938).

17. C. R. Wronski, B. Abeles, C. T. Cody, D. Morel and T. Tiedje, 14th IEEE PVSC, San Diego California, January 1980.

18. M. P. Thekaekra, Institute of Environmental Sciences, 1974.

8. RESEARCH PARTICIPANTS

W. A. Anderson	Principal Investigator
M. K. Han	Assistant Research Professor
R. Lahri	Graduate Research Assistant (Ph.D.)
P. Sung	Graduate Research Assistant (M.S.)
M. Thayer	Undergraduate Research Assistant (Part Time)
P. Yaworsky	Undergraduate Research Assistant
P. Talarico	Technician (Part Time)
J. Bennett	Secretary (Part Time)

9. REPORTS/PUBLICATIONS/PRESENTATION

REPORTS

M. K. Han and W. A. Anderson, "Fabrication and Testing of MIS Solar Cells on a-Si:F:H," Contract Number XS-9-8041-9, February 15, 1980, Project Status Report.

M. K. Han and W. A. Anderson, "Fabrication and Testing of MIS Solar Cells on a-Si:F:H," Contract Number XS-9-8041-9, May 19, 1980, Project Status Report.

M. K. Han and W. A. Anderson, "Fabrication and Testing of MIS Solar Cells on a-Si:F:H," Contract Number XS-9-8041-9, May 19, 1980, Progress Report.

PUBLICATIONS

M. K. Han, W. A. Anderson, R. Lahri and J. Coleman, "Influence of Thin Metal Films as a Top Electrode on the Characteristics of P-I-N a-Si:H Solar Cells," Journal of Applied Physics (Accepted).

PRESENTATIONS

M. K. Han and W. A. Anderson, "Fabrication and Testing of MIS Solar Cells on a-Si:F:H," Amorphous Silicon/Materials Subcontractor's Review Meeting, April 23-25, 1980, Washington, D.C.

M. K. Han and W. A. Anderson, R. Lahri, J. Coleman and H. J. Weisman, "Current Collection Mechanisms in P-N-I Junction a-Si:H Solar Cells using Spectral Response Analysis," 1980 International Electron Device Meeting, December 8-10, 1980, Washington, D. C. (Accepted)

PRESENTATIONS (Continued)

M. K. Han, W. A. anderson, R. Lahri and J. Coleman, "Fabrication Considerations for Low Cost a-Si:H Solar Cells," 4th Annual Photovoltaic Advanced Research & Development Conf., November 18-20, 1980, Colorado Springs, Colorado.

☆U.S. GOVERNMENT PRINTING OFFICE: 1980-740-145/958